nature neuroscience

Article

https://doi.org/10.1038/s41593-024-01866-2

Propagation of pathologic α-synuclein from kidney to brain may contribute to Parkinson's disease

Received: 24 November 2022

Accepted: 5 December 2024

Published online: 23 January 2025

Check for updates

Xin Yuan[1,8], Shuke Nie[1,8], Yingxu Yang[1,8], Congcong Liu[1], Danhao Xia[1], Lanxia Meng[1], Yue Xia[2], Hua Su[3], Chun Zhang[3], Lihong Bu[4], Min Deng[1], Keqiang Ye[5], Jing Xiong[1], Liam Chen[6] & Zhentao Zhang[1,7]

The pathogenesis of Lewy body diseases (LBDs), including Parkinson's disease (PD), involves α-synuclein (α-Syn) aggregation that originates in peripheral organs and spreads to the brain. PD incidence is increased in individuals with chronic renal failure, but the underlying mechanisms remain unknown. Here we observed α-Syn deposits in the kidneys of patients with LBDs and in the kidney and central nervous system of individuals with end-stage renal disease without documented LBDs. In male mice, we found that the kidney removes α-Syn from the blood, which is reduced in renal failure, causing α-Syn deposition in the kidney and subsequent spread into the brain. Intrarenal injection of α-Syn fibrils induces the propagation of α-Syn pathology from the kidney to the brain, which is blocked by renal denervation. Deletion of α-Syn in blood cells alleviates pathology in α-Syn A53T transgenic mice. Thus, the kidney may act as an initiation site for pathogenic α-Syn spread, and compromised renal function may contribute to the onset of LBDs.

Parkinson's disease (PD) and dementia with Lewy bodies (DLB) are degenerative disorders of the central nervous system (CNS) with the pathological hallmark of phosphorylated and misfolded α-synuclein (α-Syn) deposition in Lewy bodies (LBs) and Lewy neurites (LNs)[1]. Converging evidence indicates that misfolded α-Syn propagates throughout the nervous system in a prion-like manner[2,3]. Recent pathological and imaging studies have shown that the initial pathological aggregation of α-Syn may occur in peripheral organs and invade the brain during the progression of Lewy body diseases (LBDs)[4,5], in a seemingly similar fashion to that of other major neurodegenerative disorders[6]. For instance, injection of α-Syn fibrils into the gastrointestinal tract induces the progression of α-Syn pathology from the gut to the brain[7–10], while removal of the appendix is associated with a decreased risk of PD and delay of PD onset[11].

In addition to the nervous system, α-Syn is highly expressed in red blood cells (RBCs). In fact, the concentration of α-Syn in RBCs is 1,000 times higher than that in cerebrospinal fluid (CSF)[12]. Interestingly, aggregated and phosphorylated α-Syn levels in RBCs are higher in patients with PD than in healthy individuals[13]. Considering the abundance and fragility of RBCs, particularly in patients with chronic kidney diseases (CKDs)[14], it is reasonable to predict that circulating α-Syn would be elevated in patients with impaired renal function. The kidney receives both parasympathetic cholinergic fibers from the dorsal nucleus of the vagus nerve and sympathetic innervation

[1]Department of Neurology, Renmin Hospital of Wuhan University, Wuhan, China. [2]Department of Urology, Renmin Hospital of Wuhan University, Wuhan, China. [3]Department of Nephrology, Union Hospital, Tongji Medical College, Huazhong University of Science and Technology, Wuhan, China. [4]PET–CT/MRI Center, Faculty of Radiology and Nuclear Medicine, Renmin Hospital of Wuhan University, Wuhan, China. [5]Faculty of Life and Health Sciences, Shenzhen Institute of Advanced Technology, Shenzhen, China. [6]Department of Laboratory Medicine and Pathology, University of Minnesota Medical School, Minneapolis, MN, USA. [7]TaiKang Center for Life and Medical Sciences, Wuhan University, Wuhan, China. [8]These authors contributed equally: Xin Yuan, Shuke Nie, Yingxu Yang. e-mail: zhentaozhang@whu.edu.cn

from the spinal cord[15]. Notably, recent population-based studies have independently revealed that CKDs are associated with a greater risk of PD[16–18]. Furthermore, there is a negative correlation between the estimated glomerular filtration rate and the incidence of PD[18]. However, the pathological basis for the link between renal diseases and increased risk of PD remains unknown.

In this study, we show that α-Syn deposits in the kidneys of patients with end-stage renal disease. Renal failure (RF) promotes the deposition of α-Syn in the kidney and brain of mice receiving intravenous injections of α-Syn. Intrarenal injection of α-Syn fibrils triggers the spread of α-Syn pathology from the kidney to the brain. Interestingly, deletion of α-Syn from the blood cells attenuates the progression of α-Syn pathology. Taken together, we demonstrate that the kidney is a peripheral organ that serves as an origin of pathological α-Syn.

Results

α-Syn deposits in the kidneys of patients with PD and CKD

To explore whether pathologic α-Syn is present in the kidneys of patients with synucleinopathies, we stained kidney sections from 11 patients with a clinical diagnosis of PD or DLB (Supplementary Table 1). Among them, three cases were neuropathologically confirmed to be brainstem-predominant, four were limbic (transitional) and four were neocortical (diffuse) type of LBD category[19]. Immunohistochemistry (IHC) revealed that α-Syn phosphorylated at Ser129 (pα-Syn) was present in the kidneys of 10 of the 11 patients, especially in the nerve fibers adjacent to small vessels. The pα-Syn-positive signals exhibited a granular staining pattern either by themselves or together with distinct, well-formed aggregates (Fig. 1a,b, Extended Data Fig. 1a,b and Tables 1 and 2). The specificity of the pα-Syn antibody was confirmed in *Snca* knockout (*Snca*$^{-/-}$) mouse brain sections (Extended Data Fig. 1c). Most of the pα-Syn signals colocalized with the neurofilament marker neurofilament light chain (NfL; Fig. 1c). The levels of total α-Syn were not altered in the kidneys of patients with PD (Fig. 1d,e). The deposition of pathological α-Syn in the kidney was confirmed by immunostaining with another antibody that preferentially detects pathological α-Syn (Syn303; Extended Data Fig. 1b). Not surprisingly, pα-Syn was detected in the small and large intestines, stomach and lower esophagus in all 11 patients with synucleinopathies (Extended Data Fig. 1d and Supplementary Table 2).

Furthermore, we extended our research to samples from 20 patients with CKD. The demographics and clinical characteristics of the participants were summarized in Supplementary Tables 3 and 4. The average age of the CKD patients was 47.8 ± 10.3, while that of the controls was 46.7 ± 12.8. Remarkably, α-Syn pathology was detected by both anti-pα-Syn and Syn303 antibodies in the kidneys of 17 patients who suffered from CKD (Fig. 1f and Extended Data Fig. 1e). Minor pα-Syn signals were also detected in vascular endothelial cells, as shown by double immunofluorescence staining for pα-Syn and CD31 (Extended Data Fig. 1f). The levels of total α-Syn were not altered in the kidneys of patients with CKD (Fig. 1g,h). Moreover, there were extensive thioflavin S-positive signals in the kidneys of patients with CKD, further confirming the existence of amyloid structures (Fig. 1i). Notably, in seven cases of patients with CKD with available postmortem samples of the CNS, LB- and LN-like inclusions and neurites that stained positive for pα-Syn and Syn303 were present in the spinal cord, midbrain and amygdala (Fig. 1j and Extended Data Fig. 1g). To further confirm the presence of α-Syn aggregates in the kidneys, we added kidney homogenates from patients with CKD, PD or control participants to recombinant monomeric α-Syn and monitored the aggregation of α-Syn using thioflavin T (ThT) assay. Interestingly, kidney homogenates from both patients with CKD and PD were able to seed the aggregation of α-Syn, while control kidney homogenates did not (Extended Data Fig. 1h). These results suggest that the deposition of α-Syn in the kidney and brain of patients with CKD may represent presymptomatic deposition of pathologic α-Syn.

The kidney mediates the clearance of circulating α-Syn

The kidneys have vital roles in protein metabolism. To determine whether circulating α-Syn is cleared through the kidney, we intravenously injected C57BL/6J mice with 100 μg of recombinant α-Syn monomers. The concentrations of α-Syn in the serum decreased quickly, with a half-life of only 0.564 h (Fig. 2a). Interestingly, in mice with RF, the serum half-life of α-Syn extended to 0.79 h, indicating impaired clearance (Fig. 2b). We also examined the levels of α-Syn in the urine and found that the total amount of α-Syn in the 24-h urine of control mice and RF mice was similar (41.77 ng and 59.44 ng, respectively; Fig. 2c). When the mice were injected with α-Syn preformed fibrils (PFFs), the half-lives of α-Syn species in the serum of the control mice and RF mice were 0.794 h and 1.05 h, respectively (Extended Data Fig. 2a,b). The total amounts of α-Syn species in the 24-h urine samples were 58.62 ng and 68.16 ng, respectively (Extended Data Fig. 2c). These findings imply that α-Syn in the blood is quickly degraded and only a very small proportion is excreted via urine.

Next, we investigated the distribution of α-Syn in different organs of mice that received an intravenous injection of α-Syn monomers. Thirty minutes after injection, α-Syn was detected in the renal cortex, including the glomeruli and proximal convoluted tubules and gradually decreased over time. In RF mice, α-Syn emerged more in the glomerulus and less in the proximal convoluted tubules 30 min after injection, indicating impaired filtering of α-Syn by the glomerulus (Fig. 2d,e). Interestingly, α-Syn was deposited mainly in the kidney but not in the heart, liver, spleen, lung, brain, small intestine or colon (Extended Data Fig. 2d–f). Because the renal artery and renal vein of mice are too small to operate on, to further confirm that circulating α-Syn can be cleared through the kidney, we intravenously injected rabbits with 2 mg of recombinant α-Syn and evaluated the concentrations of α-Syn in the serum collected from the renal artery and renal vein. Indeed, the concentrations of α-Syn in the renal vein were lower than those in the renal artery (Fig. 2f), suggesting that circulating α-Syn is removed when the blood flows through the kidney. Interestingly, western blot analysis revealed that the levels of CK2, a kinase that phosphorylates α-Syn, were increased in the kidneys of patients with CKD (Supplementary Fig. 1a) and mice with RF (Supplementary Fig. 1b), suggesting that CK2 may be involved in the phosphorylation of α-Syn in the kidneys.

To confirm that the kidney mediates the metabolism of α-Syn, we incubated α-Syn with homogenates prepared from various organs, including the heart, liver, spleen, lung, kidney and brain. Western blot analysis of kidney homogenates revealed that α-Syn quickly degraded, while the degradation of α-Syn was less efficient in kidney lysates from RF mice (Fig. 2g and Supplementary Fig. 1c,d). To further explore the proteases that mediate the degradation of α-Syn, we added the thrombin inhibitor 5, odanacatib (a cathepsin K inhibitor), CA-074 methyl ester (a cathepsin B inhibitor), LY3000328 (a cathepsin S inhibitor) and batimastat (a matrix metalloproteinase inhibitor) to kidney homogenates and then incubated them with recombinant α-Syn. Inhibitors of cathepsin K, B and S attenuated the degradation of α-Syn (Fig. 2h). These results indicate that α-Syn is mainly degraded by cathepsins in the kidney. We then detected the levels of circulating α-Syn in patients with CKD and control participants. Remarkably, the concentrations of α-Syn in the serum of patients with CKD were higher than those in control participants (Fig. 2i). However, the α-Syn levels in the urine of patients with CKD were not different from those in the urine of control participants (Fig. 2j). These findings indicate that the kidneys physiologically remove α-Syn from the blood and that this function is compromised in patients with CKD.

RF aggravates α-Syn pathology induced by α-Syn PFFs

It has been reported that intravenous injection of α-Syn PFFs triggers α-Syn pathology in the CNS[20]. We investigated whether chronic RF affects α-Syn pathology induced by intravenous injection of α-Syn PFFs in wild-type (WT) mice. The removal of endotoxin was confirmed before

https://doi.org/10.1038/s41593-024-01866-2

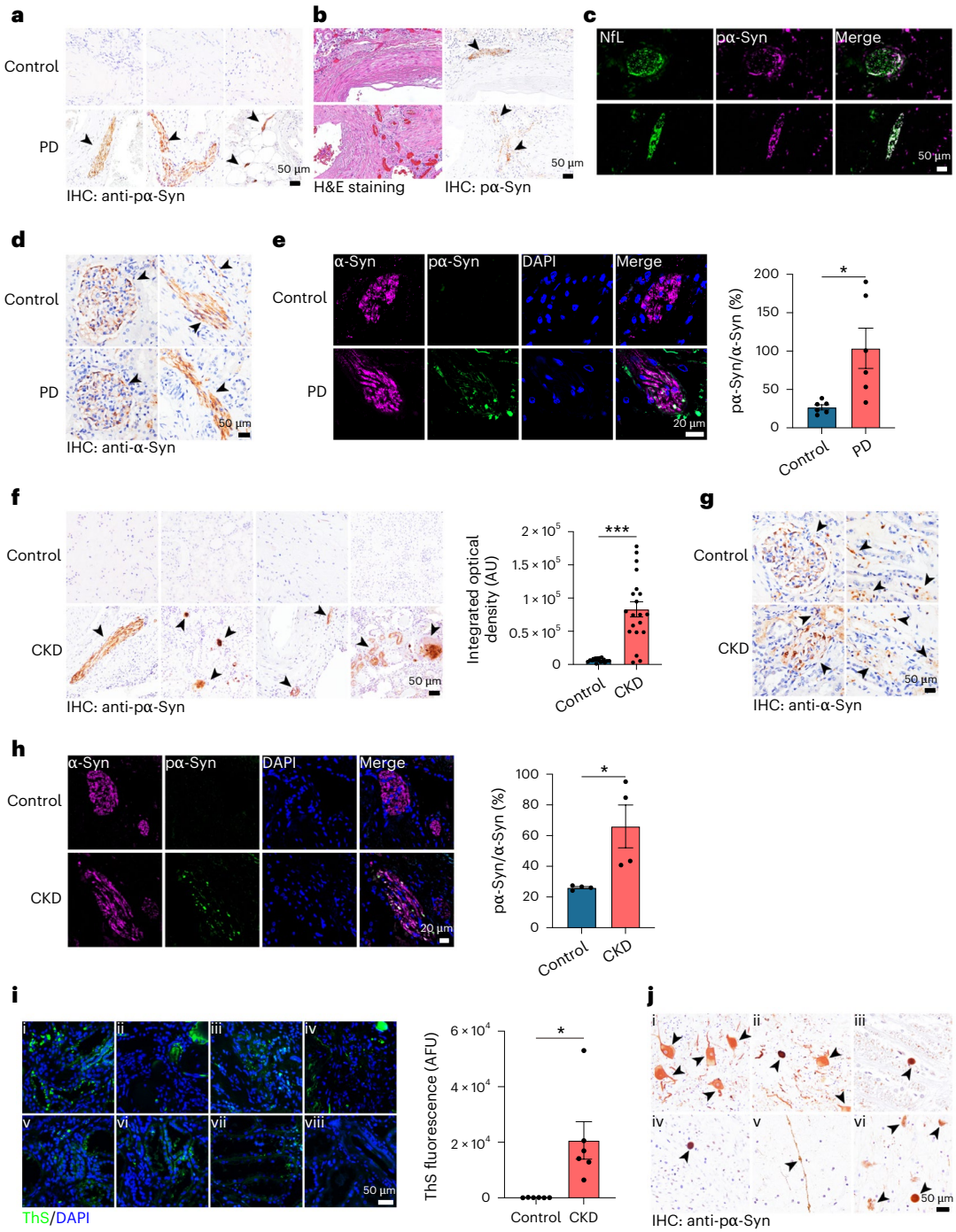

Fig. 1 | α-Syn pathology in the kidneys and CNS of patients with PD and CKD. a, IHC of pα-Syn in the kidneys of control participants and patients with PD (arrowheads, pα-Syn-positive signals). **b**, Nerve fibers (left, H&E staining) adjacent to small vessels in the kidneys were stained positive with pα-Syn antibody (right, IHC; arrowheads indicate pα-Syn-positive staining). **c**, Double immunofluorescence staining for NfL and pα-Syn in the kidneys of patients with PD. **d**, IHC of α-Syn in the kidneys of control participants and patients with PD (arrowheads, α-Syn-positive signals). **e**, Double immunofluorescence staining of α-Syn and pα-Syn in the kidneys of control participants and patients with PD ($n = 6$ independent experiments; $P = 0.0158$, unpaired two-tailed Student's t test). **f**, IHC of pα-Syn in the kidneys of control participants and patients with CKD (arrowheads show positive pα-Syn staining, $n = 17$ (control) and 20 (CKD) samples per group; $P < 0.0001$, unpaired two-tailed Student's t test). **g**, IHC of α-Syn in the kidneys of control participants and patients with CKD (arrowheads, α-Syn-positive signals). **h**, Double immunofluorescence staining for α-Syn and pα-Syn in the kidneys of control participants and patients with CKD ($n = 4$ independent experiments; $P = 0.0291$, unpaired two-tailed Student's t test). **i**, ThS staining of the kidney sections (i–vii, CKD; viii, control, $n = 6$ independent experiments; $P = 0.0123$, unpaired two-tailed Student's t test). **j**, IHC of pα-Syn in the spinal cord (i, ii), amygdala (iii, iv) and midbrain (v, vi) of patients with CKD (arrowheads, pα-Syn-positive signals). Error bars indicate the mean ± s.e.m. $^*P < 0.05$, $^{***}P < 0.001$. Scale bars = 50 µm (**a**–**d**,**f**,**g**,**i**,**j**) and 20 µm (**e**,**h**). AU, arbitrary units; AFU, arbitrary fluorescence units; ThS, thioflavin S. H&E staining, hematoxylin and eosin staining.

injection (Extended Data Fig. 3a). The morphology of the α-Syn PFFs before and after sonication was determined using transmission electron microscopy (TEM; Extended Data Fig. 3b). In addition, the presence of fibrils was confirmed by ThT fluorescence assay (Extended Data Fig. 3c), and the neurotoxicity of the PFFs we used was determined by lactate dehydrogenase (LDH) assay of cortical neurons (Extended Data Fig. 3d). Three-month-old WT mice were intravenously injected with Adriamycin to induce chronic RF, followed by repeated injections of α-Syn monomers or PFFs via the tail vein every 2 weeks for 3 months to mimic the long-term effect of elevated α-Syn under CKD conditions (Fig. 3a). Injection of Adriamycin induced RF, as indicated by destroyed glomeruli and renal tubules (Extended Data Fig. 3e), glycogen deposition (Extended Data Fig. 3f,g) and increased serum creatinine (SCr), blood urea nitrogen (BUN) and cystatin C levels (Extended Data Fig. 3h–j). Injection of α-Syn monomers did not induce pathological α-Syn in mice with normal kidneys. However, pathological α-Syn was detected in the kidney, spinal cord and brain of α-Syn monomer-injected RF mice. In mice with normal kidneys, injection of α-Syn PFFs induced α-Syn pathology around the glomerulus, with weak pathological α-Syn staining found in the spinal cord and brain. In contrast, in RF mice injected with α-Syn PFFs, abundant α-Syn deposition was found in the kidney and CNS, including the spinal cord, amygdala, hippocampus, striatum and brain cortex (Fig. 3b, Extended Data Fig. 4a,b and Supplementary Figs. 2a,b and 3a,b). The deposition of α-Syn was confirmed by western blot analysis using pα-Syn, 5G4 and Syn303 antibodies (Fig. 3c, Extended Data Fig. 4c,d and Supplementary Figs. 2c,d and 3c,d). Interestingly, pα-Syn did not colocalize with CD31 in the α-Syn-injected mice (Extended Data Fig. 3k). Furthermore, injection of α-Syn monomers or PFFs failed to induce α-Syn pathology or nigrostriatal degradation in *Snca*$^{-/-}$ mice, regardless of whether the mice had RF (Supplementary Figs. 4 and 5).

We then investigated whether RF affects the degeneration of the nigrostriatal dopaminergic pathway. Western blot analysis revealed that the levels of tyrosine hydroxylase (TH) and dopamine transporter (DAT) in the striatum were decreased in α-Syn PFF-injected RF mice (Fig. 3d,e), indicating the degeneration of dopaminergic innervation. These results were confirmed by immunohistochemical staining of striatal and substantia nigra compacta (SNc) sections (Fig. 3f,g). Consistently, the concentrations of dopamine and its metabolites were decreased in α-Syn PFF-injected RF mice (Extended Data Fig. 4e). Furthermore, behavioral tests, including the pole test, beam-walking test and footprint test, confirmed that PFF-injected RF mice exhibited motor impairments (Extended Data Fig. 4f–h).

To further validate the effect of RF on α-Syn pathology, we constructed another RF mouse model by subtotal nephrectomy and repeatedly injected the mice with α-Syn monomers or PFFs. As expected, α-Syn pathology was also elevated in mice that underwent subtotal nephrectomy (Extended Data Fig. 5a–d and Supplementary Fig. 6a). In addition, the nigrostriatal dopaminergic pathway was affected in mice that underwent subtotal nephrectomy (Supplementary Fig. 6b–d). Taken together, these results suggest that RF accelerates the spread of pathological α-Syn from the peripheral circulation to the brain in WT mice.

RF enhances α-Syn pathology in A53T mice

Next, we examined whether chronic RF affects α-Syn pathology in transgenic mice expressing the human A53T mutant α-Syn. Six-month-old hemizygous A53T transgenic mice were intravenously injected with Adriamycin to induce chronic RF. Two months later, α-Syn pathology was detected in the spinal cord, amygdala, hippocampus, cortex, SNc and striatum, but not in mice with normal kidneys (Fig. 4a, Extended Data Fig. 6a–c and Supplementary Figs. 7a,b and 8a,b). Western blot analysis using pα-Syn, Syn303 and 5G4 antibodies confirmed the presence of α-Syn pathology in the cortex of A53T mice with RF (Fig. 4b and Supplementary Figs. 7c and 8c). Furthermore, the levels of TH and DAT in the SNc were dramatically decreased in A53T mice with RF (Fig. 4c). Consistently, the density of TH-positive terminals in the striatum and the number of TH-positive neurons in the SNc were decreased (Fig. 4d,e). The concentrations of dopamine and its metabolites 3,4-Dihydroxyphenylacetic acid (DOPAC) and homovanillic acid (HVA) in the striatum were lower in A53T mice with RF than in control A53T mice (Extended Data Fig. 6d). Consistently, the motor function of the A53T mice with RF was not as good as that of the control mice (Supplementary Fig. 9a–c). These results indicate that chronic RF promotes α-Syn pathology in α-Syn A53T mice.

α-Syn pathology spreads from kidney to brain in A53T mice

To investigate whether and how α-Syn deposited in the kidney spreads to the brain, we first traced the neuronal pathways innervating the kidney by injecting Fluoro-Gold (FG) into the renal parenchyma. FG-labeled neuronal projections were found in the dorsal root ganglia (DRG), spinal cord, pons and midbrain. In the spinal cord, most of the FG signals appeared in the intermediolateral nucleus (IML). In the brain, FG-labeled neurons were found mainly in the nucleus of the solitary tract (NTS), locus coeruleus (LC), rostroventrolateral reticular nucleus (RVL), parvicellular reticular nucleus (PCRt) and paraventricular nucleus (Extended Data Fig. 7a). Next, we injected α-Syn PFFs into the cortex of the bilateral kidneys of 3-month-old hemizygous α-Syn A53T mice. One month after injection, pα-Syn was only detectable in the kidneys. Three months after injection, abundant α-Syn was detected in the CNS, including the spinal cord, LC, SNc, amygdala, hippocampus, striatum, cortex and olfactory bulb (Fig. 5a, Extended Data Fig. 8a–d and Supplementary Figs. 10a,b and 11a,b). To determine whether pathological α-Syn colocalizes with the neuronal pathways innervating the kidney, we injected pseudorabies virus (PRV) into the kidneys 3 months after the injection of α-Syn PFFs. The PRV spreads retrogradely along nerve fibers and visualizes kidney innervation. Immunofluorescence staining revealed that pα-Syn colocalized with PRV in the key nuclei of the neuronal pathways innervating the kidney, including the IML, RVL, LC and PCRt (Extended Data Fig. 7b). To further confirm the role of the neuronal pathways in the spreading of α-Syn pathology, we injected

Fig. 2 | Physiological clearance of α-Syn by the kidney. a–**c**, Mice with normal kidneys (**a**) or RF (**b**) were intravenously injected with recombinant human α-Syn monomers. The concentrations of human α-Syn in the serum and urine were determined at different times after injection. **c**, Total α-Syn in the 24-h urine of mice injected with α-Syn monomers ($n = 5$ mice per group; $P = 0.0023$ (control PBS versus control α-Syn), $P < 0.0001$ (RF PBS versus RF α-Syn), $P = 0.2127$ (control α-Syn versus RF α-Syn), two-way ANOVA). **d**,**e**, IHC showing the deposition of human α-Syn in the kidneys of mice intravenously injected with PBS or α-Syn monomers at different time points ($n = 5$ mice per group; $P < 0.0001$ (mice with RF), $P < 0.0001$ (control mice) compared with α-Syn density at 72 h after injection, one-way ANOVA). **f**, The concentrations of human α-Syn in the RA and RV of rabbits injected with recombinant human α-Syn ($n = 5$ rabbits per group; $P = 0.0106$, unpaired two-tailed Student's *t* test). **g**, Western blots showing α-Syn after incubation with homogenates prepared from various organs derived from mice with or without RF ($n = 5$ independent experiments; $P < 0.0001$ (control 0 min versus control 20 min), $P < 0.0001$ (control 0 min versus control 30 min), $P = 0.0011$ (RF 0 min versus RF 20 min), $P < 0.0001$ (RF 0 min versus RF 20 min), one-way ANOVA). **h**, Western blot analysis showing the degradation of α-Syn in kidney homogenates in the presence of different protease inhibitors ($n = 5$ independent experiments; $P < 0.0001$ (vehicle versus odanacatid 100 μM), $P < 0.0001$ (vehicle versus CA-074 100 μM), $P < 0.0001$ (vehicle versus LY3000328 100 μM), one-way ANOVA). **i**,**j**, The concentrations of α-Syn in the serum (**i**) and urine (**j**) of patients with or without CKD ($n = 30$ (control) and 37 (CKD) participants per group; $P = 0.0004$ (**i**), $P = 0.2964$ (**j**), unpaired two-tailed Student's *t* test). Error bars indicate the mean ± s.e.m. All box-and-whisker plots depict the median, quartiles and range. $^{*}P < 0.05$, $^{**}P < 0.01$, $^{***}P < 0.001$, $^{\#\#}P < 0.01$, $^{\#\#\#}P < 0.001$. Scale bar = 20 μm (**d**). NS, not significant; RA, renal artery; RV, renal vein.

https://doi.org/10.1038/s41593-024-01866-2

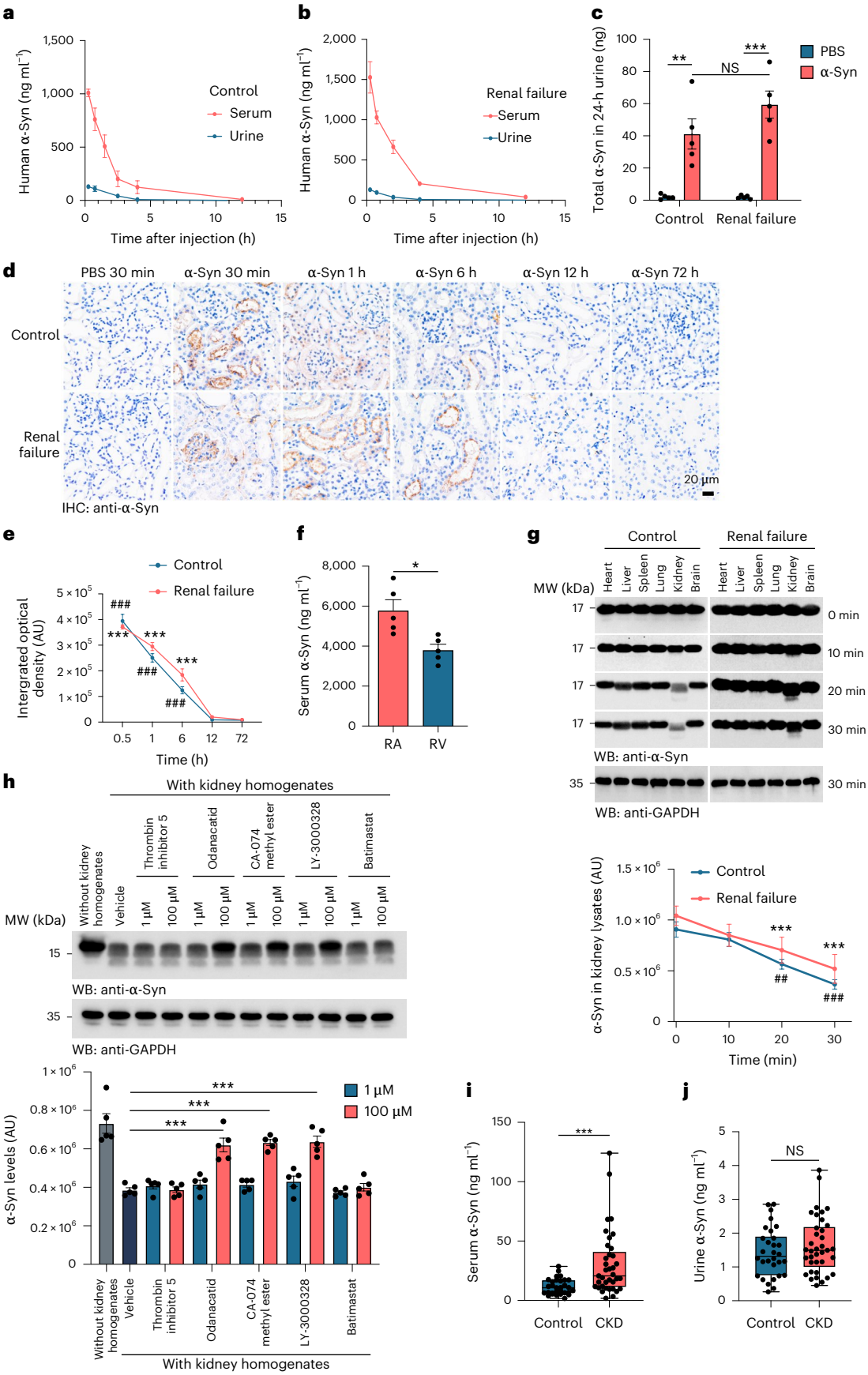

https://doi.org/10.1038/s41593-024-01866-2

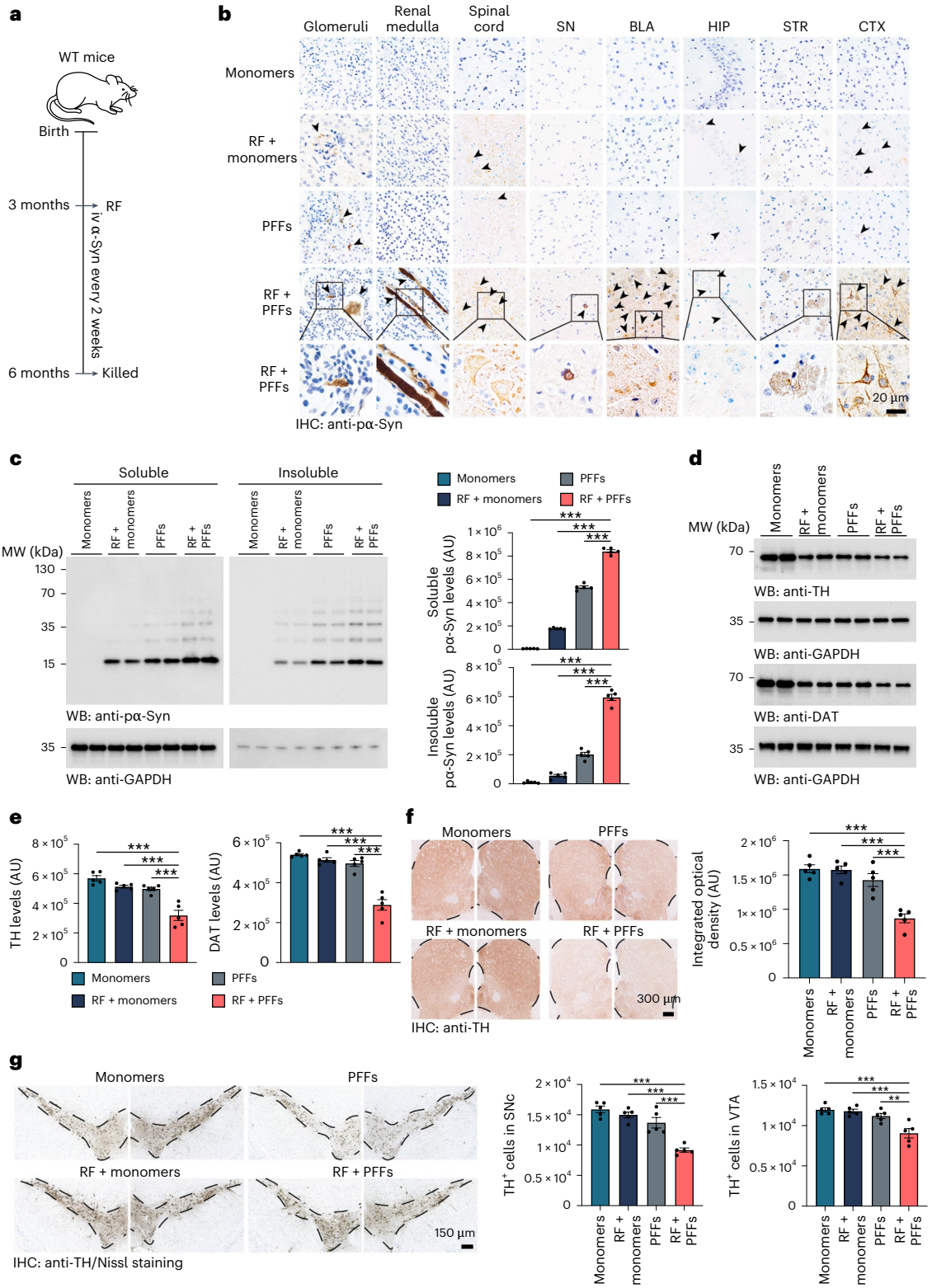

Fig. 3 | RF exacerbates α-Syn pathology induced by intravenous injection of α-Syn PFFs. a, Timeline of the experiments. **b**, Deposition of pα-Syn in the kidney, spinal cord, SN, BLA, HIP, STR and CTX of control mice or mice with RF that were injected with α-Syn monomers or PFFs. **c**, Western blot analysis of pα-Syn in the brain cortex of control mice or mice with RF that were injected with α-Syn monomers or PFFs ($n = 5$ mice per group; $P < 0.0001$, one-way ANOVA). **d**, Western blot analysis of TH and DAT in the striatum of mice. **e**, Quantification of Western blot analysis in **d** ($n = 5$ mice per group; $P < 0.0001$, one-way ANOVA). **f**, IHC of TH in the striatum of mice ($n = 5$ mice per group; $P < 0.0001$ (monomers versus RF + PFFs, RF + monomers versus RF + PFFs), $P = 0.0002$ (PFFs versus RF + PFFs), one-way ANOVA). **g**, IHC of TH and Nissl staining showing the number of TH-positive dopaminergic neurons in the SNc and VTA. Shown are the numbers of total TH-positive cells on both sides ($n = 5$ mice per group; left—$P < 0.0001$ (monomers versus RF + PFFs, RF + monomers versus RF + PFFs), $P = 0.0003$ (PFFs versus RF + PFFs), right—$P = 0.0003$ (monomers versus RF + PFFs), $P = 0.0005$ (RF + monomers versus RF + PFFs), $P = 0.0049$ (PFFs versus RF + PFFs), one-way ANOVA). Arrowheads indicate pα-Syn-positive signals (**b**). Error bars indicate the mean ± s.e.m. $^{**}P < 0.01$, $^{***}P < 0.001$. Scale bars = 20 μm (**b**), 150 μm (**g**) and 300 μm (**f**). BLA, basolateral amygdala; HIP, hippocampus; STR, striatum; CTX, cortex.

https://doi.org/10.1038/s41593-024-01866-2

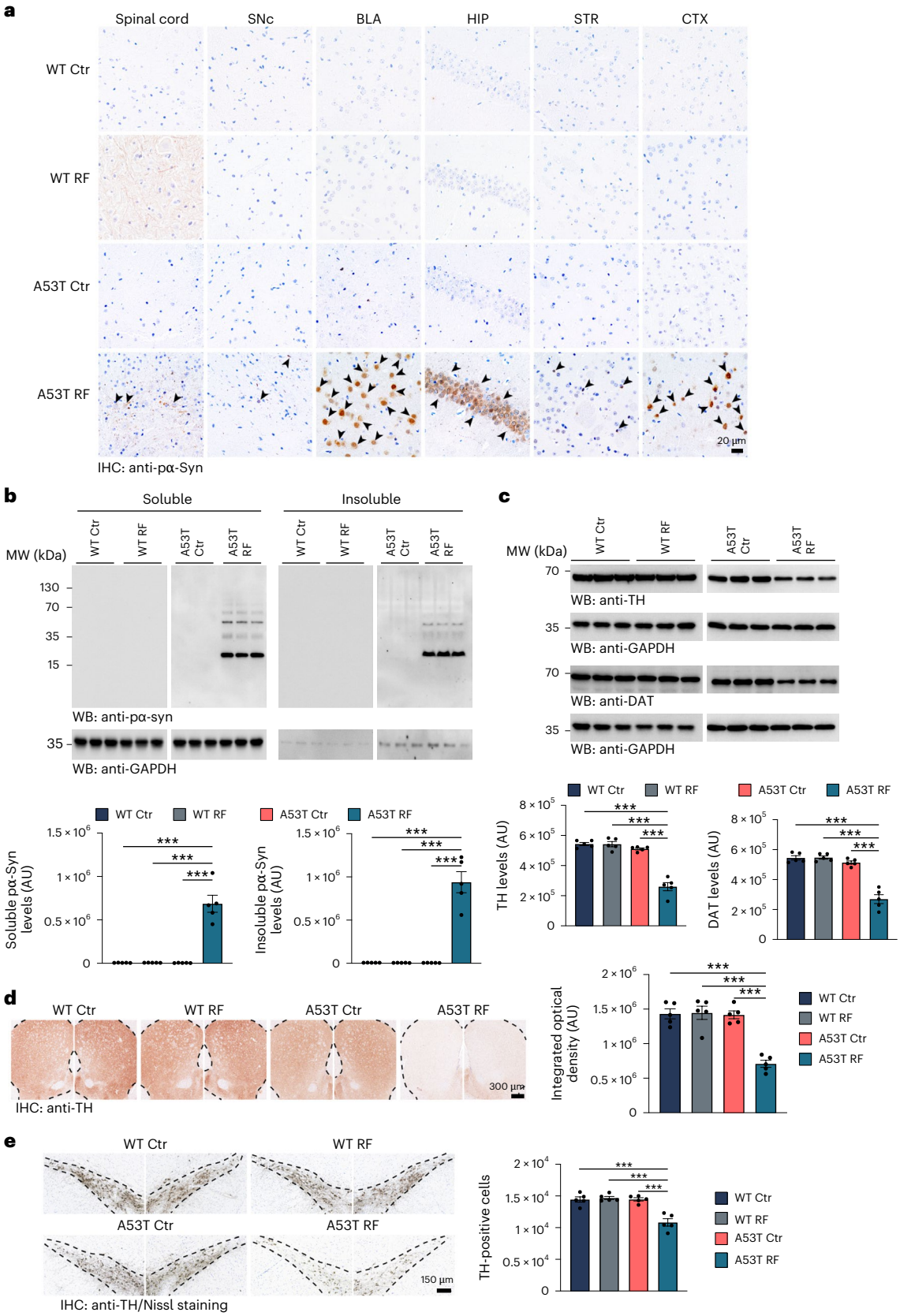

Fig. 4 | RF promotes α-Syn pathology in α-Syn A53T mice. a, IHC of pα-Syn in the spinal cord, SNc, BLA, HIP, STR and CTX of WT or α-Syn A53T mice with or without RF. **b**, Western blot analysis of pα-Syn in the cerebral cortex of mice with or without RF (the samples were derived from the same experiment, and the blots were processed in parallel. $n = 5$ mice per group; $P < 0.0001$, one-way ANOVA). **c**, Western blot analysis of TH and DAT in the striatum (the samples were derived from the same experiment, and the blots were processed in parallel. $n = 5$ mice per group; $P < 0.0001$, one-way ANOVA). **d**, IHC of TH in the striatum of mice with or without RF ($n = 5$ mice per group; $P < 0.0001$, one-way ANOVA). **e**, IHC of TH and Nissl staining showing the number of TH-positive dopaminergic neurons in the SNc. Shown are the numbers of total TH-positive cells on both sides ($n = 5$ mice per group; $P < 0.0001$, one-way ANOVA). Arrowheads, pα-Syn-positive signals (**a**). Error bars indicate the mean ± s.e.m. ***$P < 0.001$. Scale bars = 20 μm (**a**), 300 μm (**d**) and 150 μm (**e**). Ctr, control.

α-Syn PFFs into mice with renal denervation. Strikingly, α-Syn pathology was found only in the kidney but not in the spinal cord or brain in these mice (Fig. 5a, Extended Data Fig. 8a–c and Supplementary Figs. 10a,b and 11a,b). Sequential extraction of the spinal cord, cortex, midbrain and pons confirmed that intrarenal injection of α-Syn PFFs induced the formation of high-molecular-weight α-Syn species in the CNS, which was blocked by renal denervation (Fig. 5b,c and Supplementary Figs. 10c,d, 11c,d and 12a–f). Renal denervation was confirmed by immunostaining with an anti-PGP9.5 antibody (Supplementary Fig. 13). These results indicate that pathological α-Syn spreads from the kidney to the brain via the neuronal pathways innervating the kidney, leading to widespread α-Syn pathology in the CNS.

Intrarenal injection of α-Syn PFFs induces neurodegeneration

Next, we evaluated the changes in the nigrostriatal dopaminergic pathway 3 months after intrarenal injection of α-Syn PFFs. Substantial loss of TH-positive neurons in the SNc was observed in mice injected with α-Syn PFFs (Fig. 5d). Consistently, the density of TH-positive dopaminergic projections in the striatum was decreased by 72.5% in α-Syn PFF-injected A53T α-Syn transgenic mice (Fig. 5e). The levels of TH and DAT in the striatum were dramatically decreased in mice injected with α-Syn PFFs (Fig. 5f). Consistently, the levels of dopamine and its metabolites DOPAC and HVA in the striatum were decreased in mice injected with α-Syn PFFs but were attenuated in mice subjected to renal denervation (Supplementary Fig. 12g).

We then investigated the motor functions of mice that received intrarenal injections of α-Syn PFFs. A53T mice injected with α-Syn PFFs exhibited motor impairments at 3 months after injection. In the tail suspension test, mice exhibited clasping legs rather than spreading out to both sides of their bodies. The gait and motor accuracy of the α-Syn-injected mice were substantially impaired, as shown by the results of the beam-walking test, pole test and footprint test. All these motor disorders were ameliorated in mice with renal denervation (Supplementary Fig. 12h–j). These results imply that pathological α-Syn in the kidneys spreads to the brain and induces PD-like motor deficits through kidney–brain neuronal pathways.

α-Syn pathology spreads from kidney to brain in WT mice

To investigate whether intrarenal injection of α-Syn PFFs induces α-Syn pathology in non-Tg mice, we injected α-Syn PFFs into the renal cortex of 3-month-old WT mice. Three months after injection, pathological α-Syn was only detectable in the kidney. Six months after injection, α-Syn pathology was detected in the CNS using pS129, 5G4 and S303 antibodies (Extended Data Fig. 9a,b and Supplementary Figs. 14a,b and 15a,b). Western blot analysis revealed the formation of insoluble α-Syn species in the CNS of WT mice that received intrarenal injection of PFFs (Extended Data Fig. 9c and Supplementary Figs. 14c and 15c). Moreover, the levels of TH and DAT in the striatum were decreased in mice injected with α-Syn PFFs (Supplementary Fig. 16a). Consistently, TH-positive neurons in the SNc and TH-positive dopaminergic projections in the striatum were lost in mice injected with α-Syn PFFs (Supplementary Fig. 16b,c). In addition, the PFF-injected mice exhibited poor performance in the pole test, beam-walking test and footprint test 6 months after α-Syn PFF injection (Supplementary Fig. 16d–f). Interestingly, renal denervation blocked the development of α-Syn pathology in the CNS, the loss of nigrostriatal dopaminergic neurons and PD-like motor impairments in WT mice that received intrarenal injection of α-Syn PFFs (Extended Data Fig. 9 and Supplementary Figs. 14–16). Furthermore, intrarenal injection of α-Syn PFFs failed to trigger α-Syn pathology or nigrostriatal degradation in *Snca*$^{-/-}$ mice (Supplementary Fig. 17a–f). Taken together, these results indicate that α-Syn pathology spreads from the kidneys to the brain in WT mice.

Deletion of α-Syn in RBCs ameliorates PD-like pathology

RBCs are the major source of α-Syn in blood. More than 99% of α-Syn in the blood resides in RBCs[12]. To evaluate the role of α-Syn derived from blood cells in the onset of PD pathology, we transplanted homozygous α-Syn A53T mice (8 months old) with bone marrow from *Snca*$^{-/-}$ mice to delete α-Syn in blood cells (Fig. 6a–c). The concentrations of α-Syn in the serum of mice that received *Snca*$^{-/-}$ bone marrow were substantially lower than those in the serum of mice that received WT bone marrow (Fig. 6d). Nine months after transplantation, IHC and western blot analysis showed that α-Syn pathology in the spinal cord and various brain regions was dramatically decreased in mice that received *Snca*$^{-/-}$ bone marrow compared with mice that received WT bone marrow (Fig. 6e,f and Supplementary Figs. 18a and 19a–f). In addition, the levels of TH and DAT in the striatum were higher in mice that received *Snca*$^{-/-}$ bone marrow than in mice that received WT bone marrow (Fig. 6g). Consistent with these findings, IHC revealed that the density of dopaminergic terminals in the striatum and the number of TH-positive neurons in the SNc were higher in mice that received *Snca*$^{-/-}$ bone marrow (Fig. 6h,i). These findings indicate that α-Syn from blood cells contributes to the onset and progression of α-Syn pathology in α-Syn A53T mice.

Next, we explored whether bone marrow transplantation (BMT) affects α-Syn pathology in WT RF mice. The mice were transplanted with bone marrow from WT mice or *Snca*$^{-/-}$ mice and injected with Adriamycin to induce chronic RF, followed by intravenous injection of α-Syn monomers or PFFs every 2 weeks for 3 months. α-Syn pathology was detected in the kidney and CNS. There was no difference in α-Syn pathology between mice transplanted with bone marrow from *Snca*$^{-/-}$ mice and WT mice (Extended Data Figs. 4a and 10a,b). These results indicate that exogenous α-Syn is sufficient to trigger α-Syn pathology even in the absence of endogenous erythrocytic α-Syn. We further investigated the effect of BMT in A53T mice and WT mice that received intrarenal injection of α-Syn PFFs. As expected, BMT did not affect the development of α-Syn pathology in α-Syn PFF-injected mice (Supplementary Fig. 20a,b). Taken together, these results indicate that erythrocytic α-Syn is required for the progression of α-Syn pathology in mice that did not receive exogenous α-Syn PFFs. However, once the mice are exposed to exogenous α-Syn PFFs, deletion of erythrocytic α-Syn cannot reverse α-Syn pathology.

Discussion

In the present study, we identified the kidney as a peripheral origin of CNS α-Syn pathology. Pathologic α-Syn was detected in the kidneys of patients with PD or DLB. Notably, all patients with CKD we tested had α-Syn pathology in their kidneys despite a lack of history of LBD, indicating that these are most likely presymptomatic deposition of pathologic α-Syn. These findings are in line with previous reports that CKD is associated with an increased risk of idiopathic PD[17,18,21].

α-Syn pathology in LBD is frequently observed in the peripheral nervous system[6]. It is well known that α-Syn pathology may spread from the gut to the brain through the vagus nerve[7–10]. Intramuscular injection of α-Syn fibrils also induces α-Syn pathology in the brain[22], suggesting that multiple pathways may exist for the transmission of α-Syn from the periphery to the brain. The plasma levels of α-Syn exceed those in CSF by approximately tenfold[23]. Circulating α-Syn may deposit in peripheral organs and form seeds that trigger further α-Syn aggregation. Here we show that intrarenal injection of α-Syn PFFs induces the deposition of pathological α-Syn in the kidney and CNS. It has been reported that intrarenal nerve axons make direct contact with afferent and efferent arterioles and with the epithelial basement membrane of both proximal and distal tubules[24,25]. Consistently, we found that the nerve fibers adjacent to small vessels were stained positive for pα-Syn in kidney sections from patients with LBD. Similar to the gut-to-brain α-Syn transmission model, renal nerves are mixed nerves that contain both afferent and efferent nerve fibers connecting the kidney to the brain, providing the anatomical basis for the kidney-to-brain α-Syn spreading hypothesis[26]. Intriguingly, α-Syn pathology was found in the myenteric nerve plexus of the intestine and esophagus in one patient with PD without evidence of kidney involvement. There were no

https://doi.org/10.1038/s41593-024-01866-2

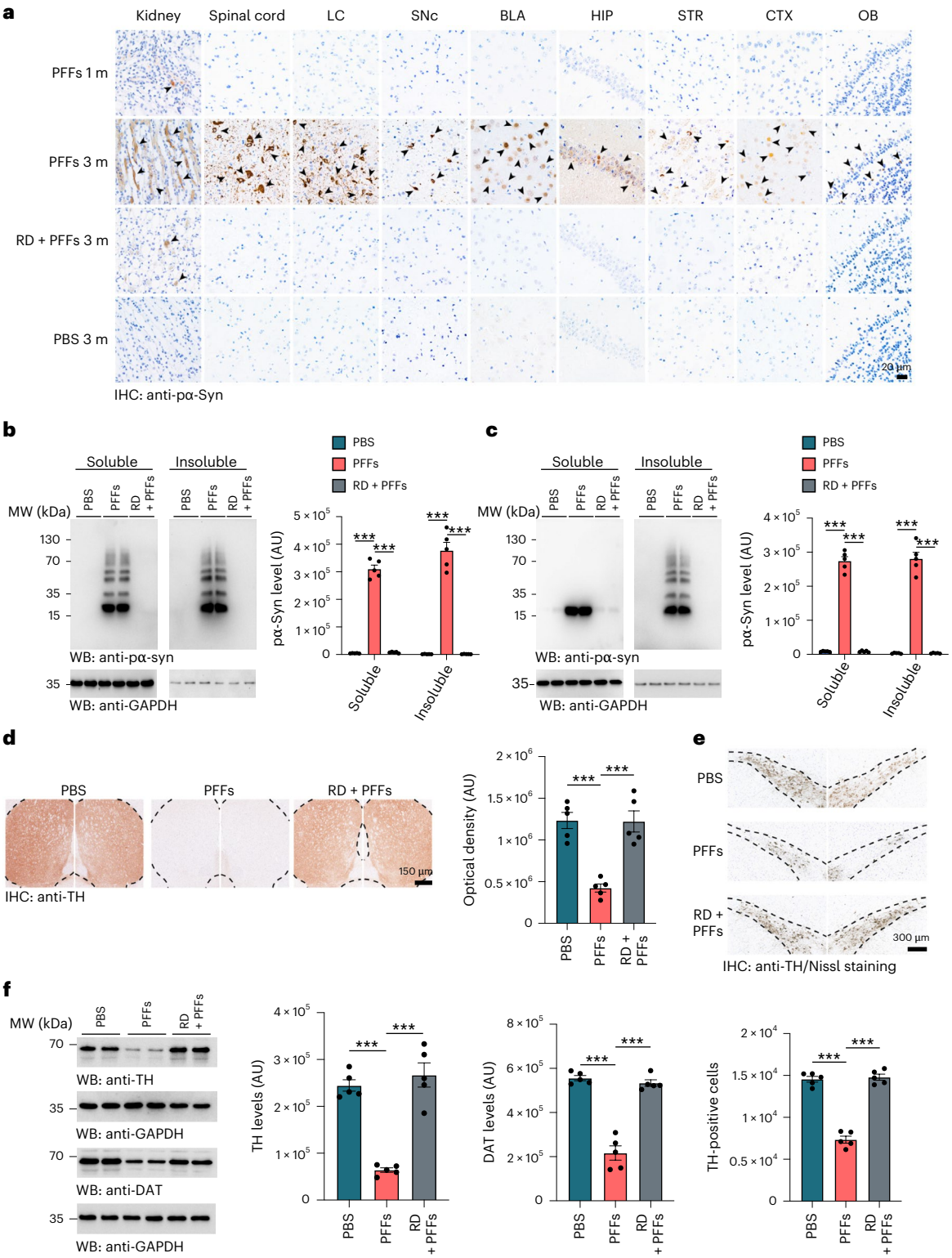

Fig. 5 | Intrarenal injection of α-Syn PFFs promotes α-Syn pathology in α-Syn A53T mice. a, IHC of pα-Syn in the kidney, spinal cord, LC, SNc, BLA, HIP, STR, CTX and OB of α-Syn A53T mice with or without RD that received intrarenal injection of PBS or α-Syn PFFs. **b**,**c**, Western blot analysis of pα-Syn in the radio immunoprecipitation assay (RIPA)-soluble and RIPA-insoluble fractions of the spinal cord (**b**) and cerebral cortex (**c**) of α-Syn A53T mice injected with PBS and α-Syn PFFs ($n = 5$ mice per group; $P < 0.0001$, one-way ANOVA). **d**, IHC of TH in the striatum of α-Syn A53T mice that received intrarenal injection of α-Syn PFFs ($n = 5$ mice per group; $P = 0.0002$ (PBS versus PFFs), $P = 0.0002$ (PFFs versus RD + PFFs), one-way ANOVA). **e**, IHC of TH and Nissl staining showing the number of TH-positive dopaminergic neurons in the SNc. Shown are the numbers of total TH-positive cells on both sides ($n = 5$ mice per group; $P < 0.0001$, one-way ANOVA). **f**, Western blot analysis of TH and DAT in the striatum ($n = 5$ mice per group; $P < 0.0001$, one-way ANOVA). Arrowheads indicate pα-Syn-positive signals (**a**). Error bars indicate the mean ± s.e.m. ***$P < 0.001$. Scale bars = 20 μm (**a**), 150 μm (**b**) and 300 μm (**d**). OB, olfactory bulb; RD, renal denervation.

https://doi.org/10.1038/s41593-024-01866-2

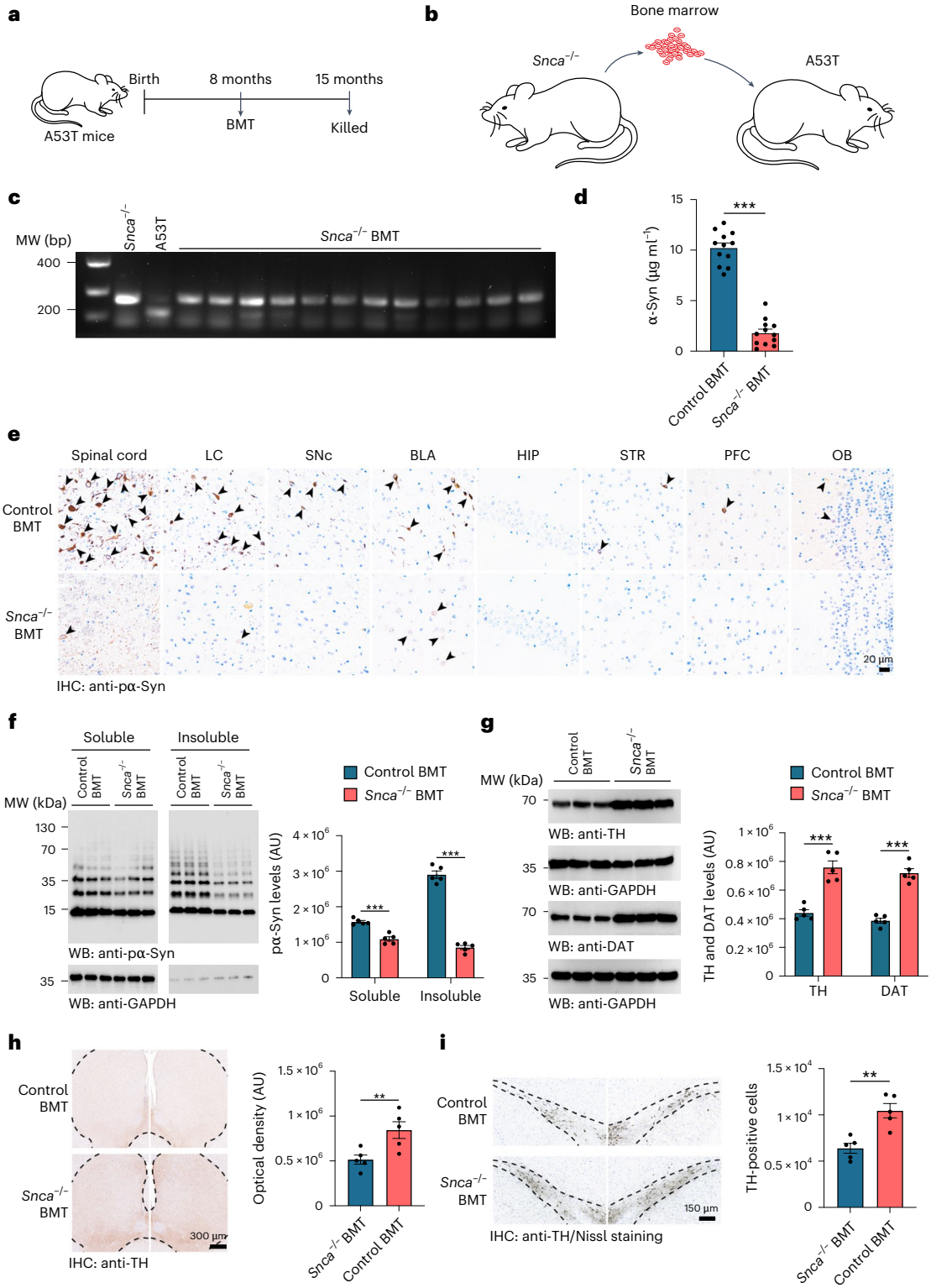

Fig. 6 | Transplantation of Snca$^{-/-}$ bone marrow ameliorates PD-like pathology in α-Syn A53T mice. a, Timeline of the experiments. **b**, Schematic diagram of BMT. **c**, Agarose gel electrophoresis showing the genotyping results of mouse blood cells after BMT. PCR products of DNA extracted from the blood cells of *Snca*$^{-/-}$ mice and α-Syn A53T mice were loaded as a control. **d**, ELISA analysis showing the α-Syn concentration in the peripheral blood of mice transplanted with bone marrow from control mice and *Snca*$^{-/-}$ mice ($n = 12$ mice per group; $P < 0.0001$, unpaired two-tailed Student's t test). **e**, IHC of pα-Syn in the spinal cord, LC, SNc, BLA, HIP, STR, CTX and OB of α-Syn A53T mice transplanted with the bone marrow of control mice and *Snca*$^{-/-}$ mice. **f**, Western blot analysis of pα-Syn in the brains of α-Syn A53T mice after transplantation (mean ± s.e.m.; $n = 5$ mice per group; $P = 0.0002$ (soluble), $P < 0.0001$ (insoluble), unpaired two-tailed Student's t test). **g**, Western blot analysis of TH and DAT in the striatum (mean ± s.e.m.; $n = 5$ mice per group; $P = 0.0002$ (TH), $P < 0.0001$ (DAT), unpaired two-tailed Student's t test). **h**, IHC of TH in the striatum (mean ± s.e.m.; $n = 5$ mice per group; $P = 0.0084$, unpaired two-tailed Student's t test). **i**, IHC of TH and Nissl staining showing the number of TH-positive dopaminergic neurons in the SNc. Shown are the numbers of total TH-positive cells on both sides (mean ± s.e.m.; $n = 5$ mice per group; $P = 0.0025$, unpaired two-tailed Student's t test). Arrowheads indicate pα-Syn-positive signals (**e**). Error bars indicate the mean ± s.e.m. $^{**}P < 0.01$, $^{***}P < 0.001$. Error bars indicate the mean ± s.e.m. $^{**}P < 0.01$, $^{***}P < 0.001$. Scale bars = 20 μm (**e**), 150 μm (**i**) and 300 μm (**h**).

substantial differences in the age of onset, disease duration or severity between this particular patient and the remaining patients, suggesting that the kidney and gastrointestinal tract are independently involved in the development of α-Syn pathology.

The kidneys have a pivotal role in protein metabolism. Proteins with molecular weights below 20 kDa freely flow through the glomerulus and are subsequently absorbed and degraded by renal tubular cells[27]. We found that the concentration of α-Syn in the renal vein was lower than that in the renal artery, suggesting that α-Syn in the blood is degraded when it circulates through the kidney. RF is associated with impaired clearance or metabolism of a variety of substances, leading to neurotoxicity and cognitive impairment[28,29]. This is thought to be related to uremic neurotoxins, changes in electrolytes and acid–base homeostasis, inflammation, etc.[30–33]. These processes may cause brain disorders. However, RF did not cause dopaminergic neurodegeneration or motor impairment in *Snca*$^{-/-}$ mice, indicating that the deposition of α-Syn has a pivotal role in motor impairment induced by chronic RF. It is conceivable that renal dysfunction may lead to impaired clearance of α-Syn and the accumulation of α-Syn in the kidneys. The pathology may progress in decades to trigger α-Syn pathology in the brain. This is supported by our observation that RF exacerbates pathology induced by intravenous injection of α-Syn PFFs in mice, resulting in dramatic α-Syn accumulation in the kidney and CNS. Interestingly, we observed that α-Syn pathology was more abundant in the brain cortex than in the SNc of mice intravenously injected with α-Syn PFFs. These results suggest that pS129-positive neurons in the SNc are lost during the progression of the disease. Furthermore, there might be other routes for the spread of peripheral α-Syn into the brain in addition to kidney-to-brain transmission. For example, circulating α-Syn may cross the blood–brain barrier to induce pathology in the CNS.

The major source of peripheral α-Syn is RBCs. Peripheral inflammation and infections increase the risk of developing PD[29,30]. Urinary tract infections have also been shown to be a risk factor for multiple system atrophy, even when the infection occurs years before diagnosis[34]. The protein level of α-Syn can be transiently elevated during infection via immune-related mechanisms or via hemolysis. Kidney function is crucial for maintaining the homeostasis of peripheral α-Syn and for dealing with the excessive α-Syn that might be produced during inflammatory events. In line with this notion, the BMT experiments presented here suggest that the systemic component of α-Syn might have been largely underappreciated.

The kidneys of a healthy adult filter approximately 180 l of blood daily. Thus, numerous RBCs are filtered by the kidneys every day[35]. RF leads to increased RBC fragmentation and intracellular protein release, possibly causing more α-Syn to deposit in the kidney[36]. Indeed, extensive α-Syn pathology was found in the kidney and CNS of patients with CKD without parkinsonism, indicating that these patients may represent the presymptomatic stage of PD or other synucleinopathies. Currently, we do not know which types of synucleinopathy are relevant. However, epidemiological evidence indicates that patients with CKD are at higher risk for PD, and a group of patients with PD develop peripheral pathology before brain pathology (brain-first PD)[37]. In addition to being degraded in the kidney, α-Syn can also be degraded in glial cells in the brain and in hepatocytes[38–40]. Dysfunction of these degradation systems may also result in α-Syn accumulation.

Taken together, the findings of the present study support that dysfunctional α-Syn clearance via the kidney may be involved in the development of α-Syn pathology in LBD. Peripheral α-Syn released from blood cell deposits in the kidney and spreads to the brain in a prion-like manner, leading to degeneration of the dopaminergic nigrostriatal pathway and LBD phenotypes. Removal of α-Syn from the blood may hinder the progression of PD, providing new strategies for therapeutic management of LBD. Although the methods used in the present study, such as BMT and renal denervation, are not practical in clinical settings, other methods that selectively eliminate circulating α-Syn, such as the administration of α-Syn-specific antibodies, may hold promise.

Online content

Any methods, additional references, Nature Portfolio reporting summaries, source data, extended data, supplementary information, acknowledgements, peer review information; details of author contributions and competing interests; and statements of data and code availability are available at https://doi.org/10.1038/s41593-024-01866-2.

References

1. Koga, S., Sekiya, H., Kondru, N., Ross, O. A. & Dickson, D. W. Neuropathology and molecular diagnosis of synucleinopathies. *Mol. Neurodegener.* **16**, 83 (2021).
2. Braak, H. et al. Staging of brain pathology related to sporadic Parkinson's disease. *Neurobiol. Aging* **24**, 197–211 (2003).
3. Ayers, J. I., Paras, N. A. & Prusiner, S. B. Expanding spectrum of prion diseases. *Emerg. Top Life Sci.* **4**, 155–167 (2020).
4. Arotcarena, M.-L. et al. Bidirectional gut-to-brain and brain-to-gut propagation of synucleinopathy in non-human primates. *Brain* **143**, 1462–1475 (2020).
5. Sharabi, Y., Vatine, G. D. & Ashkenazi, A. Parkinson's disease outside the brain: targeting the autonomic nervous system. *Lancet Neurol.* **20**, 868–876 (2021).
6. Wakabayashi, K., Mori, F., Tanji, K., Orimo, S. & Takahashi, H. Involvement of the peripheral nervous system in synucleinopathies, tauopathies and other neurodegenerative proteinopathies of the brain. *Acta Neuropathol.* **120**, 1–12 (2010).
7. Kim, S. et al. Transneuronal propagation of pathologic α-synuclein from the gut to the brain models Parkinson's disease. *Neuron* **103**, 627–641 (2019).
8. Ahn, E. H. et al. Initiation of Parkinson's disease from gut to brain by δ-secretase. *Cell Res.* **30**, 70–87 (2020).
9. Challis, C. et al. Gut-seeded α-synuclein fibrils promote gut dysfunction and brain pathology specifically in aged mice. *Nat. Neurosci.* **23**, 327–336 (2020).
10. Holmqvist, S. et al. Direct evidence of Parkinson pathology spread from the gastrointestinal tract to the brain in rats. *Acta Neuropathol.* **128**, 805–820 (2014).
11. Killinger, B. A. et al. The vermiform appendix impacts the risk of developing Parkinson's disease. *Sci. Transl. Med.* **10**, eaar5280 (2018).
12. Barbour, R. et al. Red blood cells are the major source of α-synuclein in blood. *Neurodegener. Dis.* **5**, 55–59 (2008).
13. Tian, C. et al. Erythrocytic α-synuclein as a potential biomarker for Parkinson's disease. *Transl. Neurodegener.* **8**, 15 (2019).
14. Gwoździński, K., Janicka, M., Brzeszczyńska, J. & Luciak, M. Changes in red blood cell membrane structure in patients with chronic renal failure. *Acta Biochim. Pol.* **44**, 99–107 (1997).
15. Schramm, L. P., Strack, A. M., Platt, K. B. & Loewy, A. D. Peripheral and central pathways regulating the kidney: a study using pseudorabies virus. *Brain Res.* **616**, 251–262 (1993).
16. Baek, S. H. et al. Incident Parkinson's disease in kidney transplantation recipients: a nationwide population-based cohort study in Korea. *Sci Rep.* **11**, 10541 (2021).
17. Wang, I.-K. et al. Increased risk of Parkinson's disease in patients with end-stage renal disease: a retrospective cohort study. *Neuroepidemiology* **42**, 204–210 (2014).
18. Nam, G. E. et al. Chronic renal dysfunction, proteinuria, and risk of Parkinson's disease in the elderly. *Mov. Disord.* **34**, 1184–1191 (2019).
19. McKeith, I. G. et al. Diagnosis and management of dementia with Lewy bodies: third report of the DLB Consortium. *Neurology* **65**, 1863–1872 (2005).

20. Peelaerts, W. et al. α-Synuclein strains cause distinct synucleinopathies after local and systemic administration. *Nature* **522**, 340–344 (2015).
21. Lin, S.-Y. et al. Association between acute kidney injury and risk of Parkinson disease. *Eur. J. Intern. Med.* **36**, 81–86 (2016).
22. Sacino, A. N. et al. Intramuscular injection of α-synuclein induces CNS α-synuclein pathology and a rapid-onset motor phenotype in transgenic mice. *Proc. Natl Acad. Sci. USA* **111**, 10732–10737 (2014).
23. Atik, A., Stewart, T. & Zhang, J. α-Synuclein as a biomarker for Parkinson's disease. *Brain Pathol.* **26**, 410–418 (2016).
24. Barajas, L. & Müller, J. The innervation of the juxtaglomerular apparatus and surrounding tubules: a quantitative analysis by serial section electron microscopy. *J. Ultrastruct. Res.* **43**, 107–132 (1973).
25. Müller, J. & Barajas, L. Electron microscopic and histochemical evidence for a tubular innervation in the renal cortex of the monkey. *J. Ultrastruct. Res.* **41**, 533–549 (1972).
26. Calaresu, F. R. & Ciriello, J. Renal afferent nerves affect discharge rate of medullary and hypothalamic single units in the cat. *J. Auton. Nerv. Syst.* **3**, 311–320 (1981).
27. Julian, B. A. et al. Sources of urinary proteins and their analysis by urinary proteomics for the detection of biomarkers of disease. *Proteomics Clin. Appl.* **3**, 1029–1043 (2009).
28. Tian, D.-Y. et al. Physiological clearance of amyloid-β by the kidney and its therapeutic potential for Alzheimer's disease. *Mol. Psychiatry* **26**, 6074–6082 (2021).
29. Viggiano, D. et al. Mechanisms of cognitive dysfunction in CKD. *Nat. Rev. Nephrol.* **16**, 452–469 (2020).
30. Rosner, M. H., Husain-Syed, F., Reis, T., Ronco, C. & Vanholder, R. Uremic encephalopathy. *Kidney Int.* **101**, 227–241 (2022).
31. Li, X.-Y. et al. Alterations of erythrocytic phosphorylated α-synuclein in different subtypes and stages of Parkinson's disease. *Front. Aging Neurosci.* **13**, 623977 (2021).
32. Wang, X., Yu, S., Li, F. & Feng, T. Detection of α-synuclein oligomers in red blood cells as a potential biomarker of Parkinson's disease. *Neurosci. Lett.* **599**, 115–119 (2015).
33. Wang, L. et al. A comparative study of the diagnostic potential of plasma and erythrocytic α-synuclein in Parkinson's disease. *Neurodegener. Dis.* **19**, 204–210 (2019).
34. Peelaerts, W. et al. Urinary tract infections trigger synucleinopathy via the innate immune response. *Acta Neuropathol.* **145**, 541–559 (2023).
35. Chung, J.-J. et al. Albumin-associated free fatty acids induce macropinocytosis in podocytes. *J. Clin. Invest.* **125**, 2307–2316 (2015).
36. Antonelou, M. H. et al. Oxidative stress-associated shape transformation and membrane proteome remodeling in erythrocytes of end stage renal disease patients on hemodialysis. *J. Proteomics* **74**, 2441–2452 (2011).
37. Horsager, J. et al. Brain-first versus body-first Parkinson's disease: a multimodal imaging case–control study. *Brain* **143**, 3077–3088 (2020).
38. Reyes, J. F. et al. Accumulation of α-synuclein within the liver, potential role in the clearance of brain pathology associated with Parkinson's disease. *Acta Neuropathol. Commun.* **9**, 46 (2021).
39. Scheiblich, H. et al. Microglia jointly degrade fibrillar α-synuclein cargo by distribution through tunneling nanotubes. *Cell* **184**, 5089–5106 (2021).
40. Yang, Y. et al. Therapeutic functions of astrocytes to treat α-synuclein pathology in Parkinson's disease. *Proc. Natl Acad. Sci. USA* **119**, e2110746119 (2022).

Methods

Animals

All animal procedures were approved by the Institutional Animal Care and Use Committee (IACUC; WDRM 20191210). The α-Syn A53T mice (line M83) and *Snca*$^{-/-}$ mice were obtained from the Jackson Laboratory (stocks: 004479 and 003692, respectively). C57BL/6J mice and rabbits were purchased from the Hubei Provincial Center for Disease Control and Prevention. Only male mice and rabbits (12 weeks) were used in the experiments. Animals were housed and maintained under specific pathogen-free conditions with free access to water and food in the Animal Experiment Center of Renmin Hospital of Wuhan University. The animals were randomly assigned to each group.

Human tissue samples

This study was approved by the institutional review board (IRB00101384). PD and DLB cases were selected from a tertiary hospital autopsy service database from 2013 to 2018 with the following inclusion criteria: (1) participants had been evaluated and followed by movement disorder specialists and had confirmed clinical diagnosis of either PD or DLB, (2) confirmed neuropathological diagnosis of LBD pathology and (3) adequate paraffin-embedded tissue available from the brain, kidney, large intestine, small intestine, stomach and esophagus. All CKD cases fulfilled the following inclusion criteria: (1) age under 60 years old, (2) history of CKD over 3 years, (3) pathologically confirmed end-stage renal disease changes, (4) no history record of neurological disorders and (5) neuropathologically unremarkable brain except having atherosclerosis and hypoxic–ischemic changes. All the control cases had no medical history of neurological disorders or renal disease, and pathological examinations of both the brain and kidney were unremarkable. Five of eight patients with LBD who had complete medical records had constipation, which is common in patients with LBD. All patients or their proxies provided written informed consent for a brain autopsy, and the use of the material and clinical information for research purposes was obtained.

Reagents

The following antibodies and reagents were used: α-Syn (Thermo Fisher Scientific, MA5-12272), α-Syn (BD Biosciences, 610786), pα-Syn (Ser129; BioLegend, 825701), pα-Syn (Ser129; Cell Signaling Technology, 23706s), TH (Sigma-Aldrich, AB152), DAT (Proteintech, 22524-1-AP), ubiquitin (Santa Cruz Biotechnology, Sc-8017), Syn303 (BioLegend, MMS-5091), 5G4 (Sigma, MABN389), CK2α (Proteintech, 2656), GAPDH (Proteintech, 60004-1-Ig), horseradish peroxidase (HRP)-conjugated antimouse immunoglobulin G (IgG; Bio-Rad, 170-6516), HRP-conjugated antirabbit IgG (Bio-Rad, 170-6515), Alexa Fluor 594-conjugated goat antimouse IgG (Invitrogen, A-11005), Alexa Fluor 488-conjugated goat antirabbit IgG (Invitrogen, A-11012), 4′,6-diamidino-2-phenylindole dihydrochloride (DAPI; Biofroxx, EZ3412B205), FG (Fluorochrome, Denver), human α-Syn ELISA kit (ThermoFisher Scientific, KHB0061), RIPA buffer (Beyotime, P0013B), NP-40 (Beyotime, P0013F), high-efficiency IHC detection kit (ZSGB-BIO, SP-9001, SP-9002), high-capacity endotoxin removal kit (Xiamen Bioendo Technology, ER0015), recombinant cascade reagents chromogenic endotoxin quantitation kit (Xiamen Bioendo Technology, RCR0428), LDH cytotoxicity assay kit (ThermoFisher Scientific, C20301), Nissl staining kit (Solarbio, G1436), periodic acid–Schiff (PAS) staining kit (Solarbio, G1281), creatinine assay kit (Abcam, ab65340), urea nitrogen (BUN) colorimetric detection kit (ThermoFisher Scientific, EIABUN) and cystatin C quantikine ELISA kit (R&D Systems, MSCTC0).

Purification and aggregation of recombinant α-Syn

Purification of recombinant α-Syn was performed as previously described[41]. His-tagged α-Syn was expressed in *Escherichia coli* BL21 (DE3) cells. The bacteria were collected by centrifugation at 8,228*g* for 6 min. After being resuspended in 100 ml of osmotic shock buffer (30 mM Tris–HCl, 40% sucrose and 2 mM ethylenediaminetetraacetic acid disodium (pH 7.2)), the mixture was centrifuged at 18,500*g* for 20 min. The pellets were then quickly resuspended in 90 ml of cold water supplemented with 37.5 µl of saturated $MgCl_2$ and centrifuged at 18,500*g* for 20 min. Next, the supernatants were subjected to Ni-chelating affinity chromatography and eluted with 125 mM imidazole. Purified α-Syn was subsequently applied to high-capacity endotoxin removal kits to remove endotoxin. The removal of endotoxin was confirmed using a recombinant cascade reagent chromogenic endotoxin quantitation kit (Supplementary Fig. 4a). After lyophilization, the α-Syn monomers were stored at −80 °C. α-Syn PFFs were prepared by incubating α-Syn monomers (1 mg ml^{-1}) at 37 °C with constant shaking at 1,000 rpm for 5 days. Protein fibrillization was confirmed by ThT fluorescence assay and TEM. α-Syn PFFs were sonicated for 40 min before use.

ThT fluorescence of α-Syn aggregation

α-Syn monomers (1 mg ml^{-1}) were incubated with kidney lysates. The kinetics of fibrillization were measured by ThT fluorescence assay. Ten microliters of the incubation mixture were taken at various time points and diluted in 90 µl of PBS. Then, 3 µl of 10 mM ThT was added to the samples immediately before the assay. The fluorescence was recorded at 450 nm excitation and 510 nm emission wavelengths using a SpectraMax microplate reader (Molecular Devices).

Primary neuron cultures

Primary mouse cortical neurons dissected from α-Syn A53T and WT mouse embryos were cultured as previously described[42]. Neurons cultured for 7 days in vitro were used in the experiments. To evaluate the toxicity of α-Syn PFFs, we added human and mouse α-Syn PFFs to the culture medium of primary neurons for 7 days. One week later, the neurons were subjected to a cell activity assay.

LDH assay

The activity of the neurons was measured by the LDH assay kit. After incubating with α-Syn PFFs, the medium was added to a new 96-well plate. After incubation for 30 min at room temperature, the absorbance was measured at 490 nm and 680 nm using a SpectraMax microplate reader (Molecular Devices). The LDH activity was calculated as follows: (absorbance of sample hole − absorbance of the control hole)/(absorbance of the standard hole − absorbance of the standard blank hole).

Chronic RF modeling

Chronic RF in the mice was induced by intravenous injection of Adriamycin (18 mg kg^{-1} body weight)[43]. To confirm the RF mice model was successful, we performed hematoxylin and eosin (H&E) staining and PAS staining, as well as monitored the SCr, BUN and cystatin C levels following the method of the kit instructions. Four weeks after Adriamycin injection, the mice were injected with 20 µg of α-Syn monomers or PFFs through the tail vein every 2 weeks. The dose was chosen because the concentration of α-Syn in whole blood is approximately 13 µg ml^{-1} (ref. 12), and the blood volume of each mouse is approximately 1.5 ml. Thus, each mouse contains approximately 20 µg of α-Syn in the blood.

Subtotal nephrectomy modeling

A subtotal 5/6 nephrectomy was conducted as previously described[44]. Mice were anesthetized with isoflurane. A midline abdominal incision was made to expose the left kidney. After careful separation of the perirenal fat, connective tissue, adrenal gland and ureter, a 3-0 silk suture was placed circumferentially around the upper and lower poles of the left kidney, and ligature was performed. Nephrectomy of the right kidney was performed 7 days after the first operation. Briefly, the right kidney was carefully isolated and extirpated by transecting the vessels and ureter immediately distal to the ligature. The sham surgery group

also underwent two-step surgeries but without pole ligation of the left kidney or right kidney resection.

Retrograde tracing of renal innervation

To retrogradely label the neural pathways innervating the kidney, C57BL/6J mice were anesthetized with isoflurane, and retroperitoneal incisions were made to expose the bilateral kidneys. The FG (15 µl on each side) injections were carried out at three sites in the renal parenchyma using a 10 µl Hamilton syringe connected to a 30-gauge needle. FG was injected slowly until the renal surface became distinctly colored. Then, the tip of the needle was kept in situ for 2 min, and a drop of glycerin was applied to cover the pinhole. The skin was sutured and cleaned with saline-soaked swabs. Seven days later, the mice were anesthetized and perfused with 4% paraformaldehyde. The kidney, DRG, spinal cord and brain were removed and postfixed in 4% paraformaldehyde containing 30% sucrose for 24 h. The sections were cut at 20 µm using a freezing microtome and cover-slipped with glycerol. Images were captured by an Olympus IX73 microscope with a DP80 Olympus digital camera.

Generation of PRV

Optimized PRV was prepared by BrainVTA[45]. Briefly, the PS529 plasmid was generated by inserting the CAG promoter, β-globin intron, three copies of enhanced GFP, woodchuck hepatitis virus post-transcriptional regulatory element and bovine growth hormone polyadenylation signal into the IgG location of the PRV Bartha genome. Two micrograms of the PS529 plasmid were transfected into BHK21 cells. Six hours later, the transfected BHK21 cells were infected with the PRV Bartha strain at a multiplicity of infection = 1. The PRV531 virus was purified by isolating Enhanced Green Fluorescent Protein (EGFP)-positive plaques for four rounds. The virus can infect neurons and retrogradely transport in neural circuits, visually labeling the neural networks.

Intrarenal injection of α-Syn PFFs

Mice were anesthetized with isoflurane, and a retroperitoneal incision was made to expose the kidney. α-Syn PFFs (20 µg) were injected into three sites on each renal parenchyma using a 10 µl Hamilton syringe connected to a 30-gauge needle. Each mouse received an injection of 40 µg of α-Syn PFFs in total. The dose was chosen based on previous reports that 25–48 µg of PFFs can trigger α-Syn pathology when injected into the mouse gut[7,46]. The injection was carried out slowly, and the tip of the needle was kept in situ for 2 min. A drop of glycerin was applied to cover the pinhole. The skin was subsequently sutured and cleaned with saline-soaked swabs. To visualize the nerves innervating the kidneys, mice were anesthetized and injected with PRV in the renal parenchyma. Mice were perfused with 4% paraformaldehyde 7 days after PRV injection.

Mouse renal denervation

Renal denervation was performed as previously described[47]. Briefly, the renal artery and vein were dissected from the surrounding connective tissue. The visible nerves were cut off carefully. Then, the renal vessels were painted with sterile gauze soaked in 10% phenol anhydrous ethanol solution for 2 min to exterminate the remaining nerves. Renal denervation was confirmed by immunostaining with PGP9.5, a marker of nerve fibers.

BMT

BMT was carried out as previously described[48]. To prepare bone marrow cells, 12-week-old mice were killed by cervical dislocation, and the femurs and tibias were collected. After dissecting and cleaning the bones, the medullary cavities were flushed with a serum-free Dulbeccos Modified Eagle Medium/Nutrient Mixture F-12 (DMEM/F12) medium. A single-cell suspension was produced by passing the bone marrow suspension through a sterile 70-µm cell strainer. Then, the filtrate was centrifuged at 60*g* for 5 min and resuspended in PBS. Bone marrow cells (2×10^6 cells per 200 µl) were intravenously injected into the recipient mice using 1 ml syringes. Before BMT, 8-month-old α-Syn A53T recipient mice received busulfan (20 mg kg^{-1} d^{-1} × 4 days) and cyclophosphamide (100 mg kg^{-1} d^{-1} × 2 days) combination conditioning therapy. After 1 day of recovery, bone marrow cells were injected into the recipient mice. All mice were administered water containing ampicillin–streptomycin for 3 weeks to prevent bacterial infection.

IHC and immunofluorescence

Paraffin-embedded sections were deparaffinized in xylene and then hydrated through descending ethanol. After being steeped in antigen retrieval buffer (0.1 M sodium citrate (pH 6.0)) for 20 min at 94 °C, the sections were incubated with 3% H_2O_2 for 10 min to eliminate endogenous peroxidase activity. The sections were subsequently blocked in 5% bovine serum albumin and incubated with primary antibodies overnight at 4 °C. Signals were developed with a high-efficiency IHC detection kit. For immunofluorescence staining, Alexa Fluor 488- or 594-conjugated secondary antibodies were applied. Cell nuclei were labeled with DAPI. Images were captured by an Olympus DP80 microscope equipped with TH4-200 and U-HGLGPS light sources. The quantification of the integrated fluorescence intensity was performed with ImageJ software (v.2.1.0/1.53c). The person who performed the immunostainings was blinded to the diagnosis.

Thioflavin S staining of kidney sections

Human kidney sections were incubated with filtered thioflavin S solution (0.05% wt/vol in 50% ethanol) for 10 min, treated with 80% ethanol for 15 s, washed in PBS three times and observed under an Olympus DP80 microscope.

Counting of dopaminergic neurons

To determine the number of dopaminergic neurons in the substantia nigra (SN), the entire SN area of each mouse was continuously sliced into 4 µm thick paraffin sections (approximately 100–150 sections per mouse). Every sixth section was immunostained with the anti-TH antibody (approximately 20 sections per mouse). Each group contained five mice. Because six sections were 24 µm thick, which is close to the diameter of the cell body of dopaminergic neurons, the sum of the neuronal numbers in all the sections was considered the result for a single mouse. An Olympus DP80 microscope and matched software (cellSensVer1.7.1/1.8/1.9 controlling DP80) were used for cell counting.

Sequential protein extraction

RIPA-insoluble fractions were prepared as previously described[49]. Briefly, the brain tissues were homogenized in Tris Buffered Saline + (TBS+, 50 mM Tris–HCl (pH 7.4), 175 mM NaCl, 5 mM EDTA, protease inhibitor cocktail and phosphatase inhibitors) and centrifuged at 120,000*g* for 30 min at 4 °C. Then, the pellets were sequentially rinsed in TBS+ containing 1% Triton X-100, TBS+ containing 1 M sucrose and RIPA buffer. The final pellets were solubilized in 8 M urea/5% SDS, representing the RIPA-insoluble fractions containing α-Syn aggregates.

Western blots

Mouse brain tissues were lysed in RIPA lysis buffer supplemented with protease inhibitor cocktail and phosphatase inhibitor cocktail B and centrifuged at 15,550*g* for 15 min at 4 °C. The total protein content of the supernatant was quantified by a BCA assay before the samples were boiled in the SDS loading buffer. After SDS–PAGE, the proteins were transferred onto nitrocellulose membranes and incubated with the appropriate primary antibodies overnight at 4 °C. The membranes were then incubated with HRP-conjugated secondary antibodies for 1 h at room temperature. After the membranes were washed three times in Tris Buffered Saline with Tween-20 (TBST), the signals were visualized using enhanced chemiluminescence.

HPLC analysis of dopamine and its metabolites

Mouse striatal tissues were separated and snap-frozen in liquid nitrogen. Before analysis, tissues were homogenized in 0.1 M perchloric acid containing 0.1% cysteine and centrifuged at 1,8000*g* for 15 min at 4 °C. The supernatants were then filtered and analyzed via high-performance liquid chromatography (HPLC). The samples were injected into the chromatographic column (4.6 × 150 mm) and separated by a mobile phase (8% methanol in 3 mM sodium heptanesulfonate, 100 mM sodium acetate, 85 mM citric acid and 0.2 mM EDTA). The DA, DOPAC and HVA contents in each sample were quantified via comparison to the standard curve.

Behavioral tests

All behavioral tests were performed between 10:00 and 18:00 during the light-on cycles. Mice were acclimatized in the test room for 3 days. The investigators were blinded to the treatment during the behavioral tests. In the tail suspension test, the mice were suspended by hanging their tails in front of a blank background. Pictures were taken when the mice remained immobile. In the beam-walking test, a beam with a length of 80 cm and a width of 0.9 cm was used. The time for the mice to traverse 50 cm was recorded. In the pole test, the mice were placed head-upward on the top of a vertical, rough-surfaced wooden pole (1 cm diameter and 45 cm height). The following two parameters were recorded: the latency to hesitate before the mice were oriented downward and started to go down (T turn) and the total latency between the time at which the mice started to move and the time at which their paws touched the floor (T total). In the footprint test, the paws of the mice were stained with nontoxic dyes of different colors (forepaws in red and hindpaws in blue). Mice were allowed to walk through a restricted tunnel with a sheet of white paper (42 cm in length and 4.5 cm in width). Three steps from the middle portion were measured for hindlimb stride length and hind-base width.

Statistical analysis

Data are presented as mean ± s.e.m. from three or more independent experiments and analyzed by GraphPad Prism software (v.8.2.0). Unpaired Student's *t* test was used to analyze the differences between the two groups. Mann–Whitney *U* test was applied to assess the differences in the ratio between the two groups. One-way and two-way analysis of variance (ANOVA) followed by Tukey's multiple comparisons test was applied to assess the differences among three or more groups. Kruskal–Wallis test was used to assess the differences in ratios among three or more groups. Statistical significance was set as $P < 0.05$. Quantifications were performed from at least three experimental groups. The *n* value was defined as the number of experiments that were repeated independently with similar results. Data distribution was assumed to be normal, but this was not formally tested. No statistical methods were used to predetermine sample sizes, but our sample sizes were similar to those generally used in the field. No animals or data points were excluded from the analyses. Data collection and analysis were performed blinded to the conditions of the experiments and to the observers.

Reporting summary

Further information on research design is available in the Nature Portfolio Reporting Summary linked to this article.

Data availability

All data necessary for the conclusions of the study are available in 'Main', Figs. 1–6 and Extended Data Figs. 1–10. Source data are provided with this paper.

Code availability

No unique code was generated in this paper.

References

41. Pan, L. et al. Tau accelerates α-synuclein aggregation and spreading in Parkinson's disease. *Brain* **145**, 3454–3471 (2022).
42. Yuan, X. et al. Fine particulate matter triggers α-synuclein fibrillization and Parkinson-like neurodegeneration. *Mov. Disord.* **37**, 1817–1830 (2022).
43. Hayashi, K. et al. Renin-angiotensin blockade resets podocyte epigenome through Kruppel-like factor 4 and attenuates proteinuria. *Kidney Int.* **88**, 745–753 (2015).
44. Kim, K. et al. Skeletal myopathy in CKD: a comparison of adenine-induced nephropathy and 5/6 nephrectomy models in mice. *Am. J. Physiol. Renal Physiol.* **321**, F106–F119 (2021).
45. Jia, F. et al. Optimization of the fluorescent protein expression level based on pseudorabies virus Bartha strain for neural circuit tracing. *Front. Neuroanat.* **13**, 63 (2019).
46. Uemura, N. et al. Inoculation of α-synuclein preformed fibrils into the mouse gastrointestinal tract induces Lewy body-like aggregates in the brainstem via the vagus nerve. *Mol. Neurodegener.* **13**, 21 (2018).
47. Li, Q. et al. Sympathetic denervation ameliorates renal fibrosis via inhibition of cellular senescence. *Front. Immunol.* **12**, 823935 (2021).
48. Ryu, J.-H. et al. Human tonsil-derived mesenchymal stromal cells enhanced myelopoiesis in a mouse model of allogeneic bone marrow transplantation. *Mol. Med. Rep.* **14**, 3045–3051 (2016).
49. Ding, X. et al. Propagation of pathological α-synuclein from the urogenital tract to the brain initiates MSA-like syndrome. *iScience* **23**, 101166 (2020).

Acknowledgements

This work was supported by grants from the National Natural Science Foundation of China (82271447 and 81771382 to Z.Z. and 82301430 to X.Y.), the National Key Research and Development Program of China (2019YFE0115900 to Z.Z.), the Innovative Research Groups of Hubei Province (2022CFA026 to Z.Z.) and the Natural Science Foundation of Hubei Province (2021CFB451 to S.N.).

Author contributions

Z.Z. conceived and supervised the project. X.Y. performed most of the experiments. S.N., Y.X. and L.C. performed the immunostaining of human sections. Y.Y., C.L., D.X., L.M., J.X., L.B. and M.D. helped with the cell culture and animal experiments. H.S. and C.Z. collected serum and urine samples. K.Y. helped in the data interpretation.

Competing interests

The authors declare no competing interests.

Additional information

Extended data is available for this paper at https://doi.org/10.1038/s41593-024-01866-2.

Supplementary information The online version contains supplementary material available at https://doi.org/10.1038/s41593-024-01866-2.

Correspondence and requests for materials should be addressed to Zhentao Zhang.

Peer review information *Nature Neuroscience* thanks Veerle Baekelandt, Han Seok Ko and the other, anonymous, reviewer(s) for their contribution to the peer review of this work.

https://doi.org/10.1038/s41593-024-01866-2

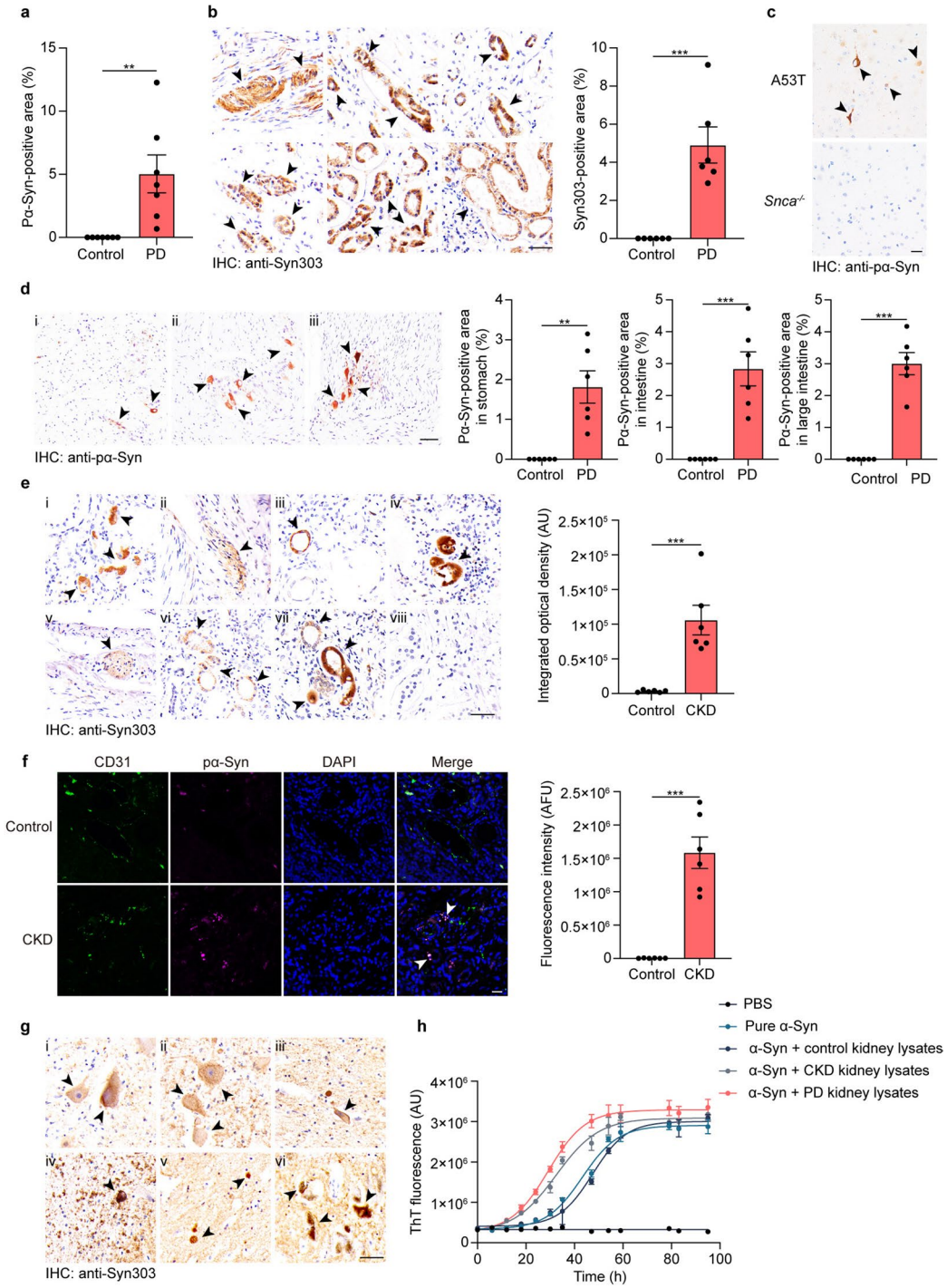

Extended Data Fig. 1 | α-Syn pathology in the kidneys, CNS and gastrointestinal tract of patients with PD and CKD. a, Quantification of immunohistochemistry in Fig. 1a showing the positive pα-Syn area in the kidneys of patients with PD (n = 7 samples per group; $P = 0.0057$). **b**, Immunohistochemistry of Syn303 antibody in the kidneys of patients with PD (arrowheads: pα-Syn-positive signals; n = 6 samples per group; P = 0.0004). **c**, Immunohistochemistry of pα-Syn in the cortex of α-Syn A53T mice and Snca−/− mice. **d**, Immunohistochemistry of pα-Syn in the stomach (i), small intestine (ii) and large intestine (iii) of patients with PD (arrowheads: pα-Syn-positive signals; n = 6 samples per group; $P = 0.0012$ (left), $P = 0.0003$ (middle), $P < 0.0001$ (right)). **e**, Immunohistochemistry of Syn303 antibody in the kidneys of patients with CKD and control subjects (i–vii: CKD, viii: control, arrowheads: pα-Syn-positive signals; n = 6 samples per group; $P = 0.0007$). **f**, Double immunofluorescence of CD31 and pα-Syn in the kidneys of patients with CKD and control subjects (arrowheads: pα-Syn-positive signals; n = 6 samples per group; $P < 0.0001$). **g**, Immunohistochemistry of the Syn303 antibody in the spinal cord (i, ii), amygdala (iii, iv) and midbrain (v, vi) of patients with CKD (arrowheads: pα-Syn-positive signals). **h,** Thioflavin T (ThT) analysis showing the fibrillization of α-Syn in the presence of kidney tissues from patients with PD or CKD and control subjects. Error bars indicate the mean ± s.e.m. $^{**}P < 0.01$, $^{***}P < 0.001$. Unpaired two-tailed Student's t-test was used. AU, arbitrary units; AFU, arbitrary fluorescence units. Scale bars: 20 μm (**b**,**f**) and 50 μm (**c**,**d**,**e**,**g**).

https://doi.org/10.1038/s41593-024-01866-2

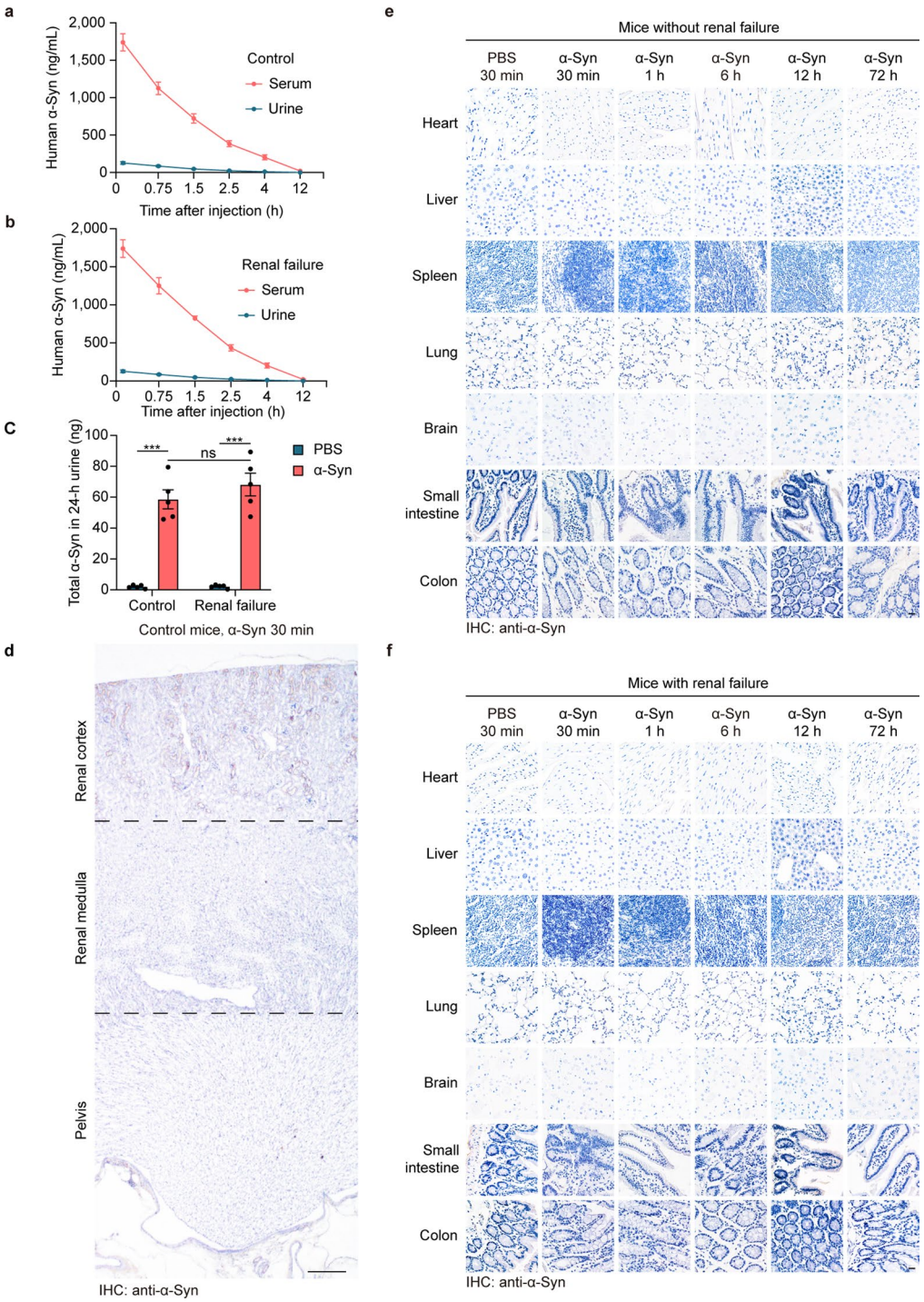

Extended Data Fig. 2 | The kidneys physiologically remove α-Syn from the blood. a,**b**, Mice with normal kidney (**a**) or renal failure (**b**) were intravenously injected with recombinant human α-Syn PFFs. The concentrations of human α-Syn in the serum and urine were determined at different times after injection. **c**, Total α-Syn in the 24-hour urine of mice injected with α-Syn or PFFs (**c**) (n = 5 mice per group, $P < 0.0001$ (control PBS vs. control α-Syn, renal failure PBS vs. renal failure α-Syn), $P = 0.5176$ (control α-Syn vs. renal failure α-Syn), error bars indicate the mean ± s.e.m; ns, not significant; ***P < 0.001, two-way ANOVA). **d**, Immunohistochemistry showing the overall distribution of human α-Syn in the kidney at 30 min after intravenous injection of human α-Syn monomers. **e**, Immunohistochemistry of human α-Syn in different organs of mice without renal failure at different time points after intravenous injection of recombinant human α-Syn monomers. **f**, Immunohistochemistry of human α-Syn in different organs of mice with renal failure at different time points after intravenous injection of recombinant human α-Syn monomers. Scale bars: 100 μm (**d**) and 20 μm (**e**,**f**).

https://doi.org/10.1038/s41593-024-01866-2

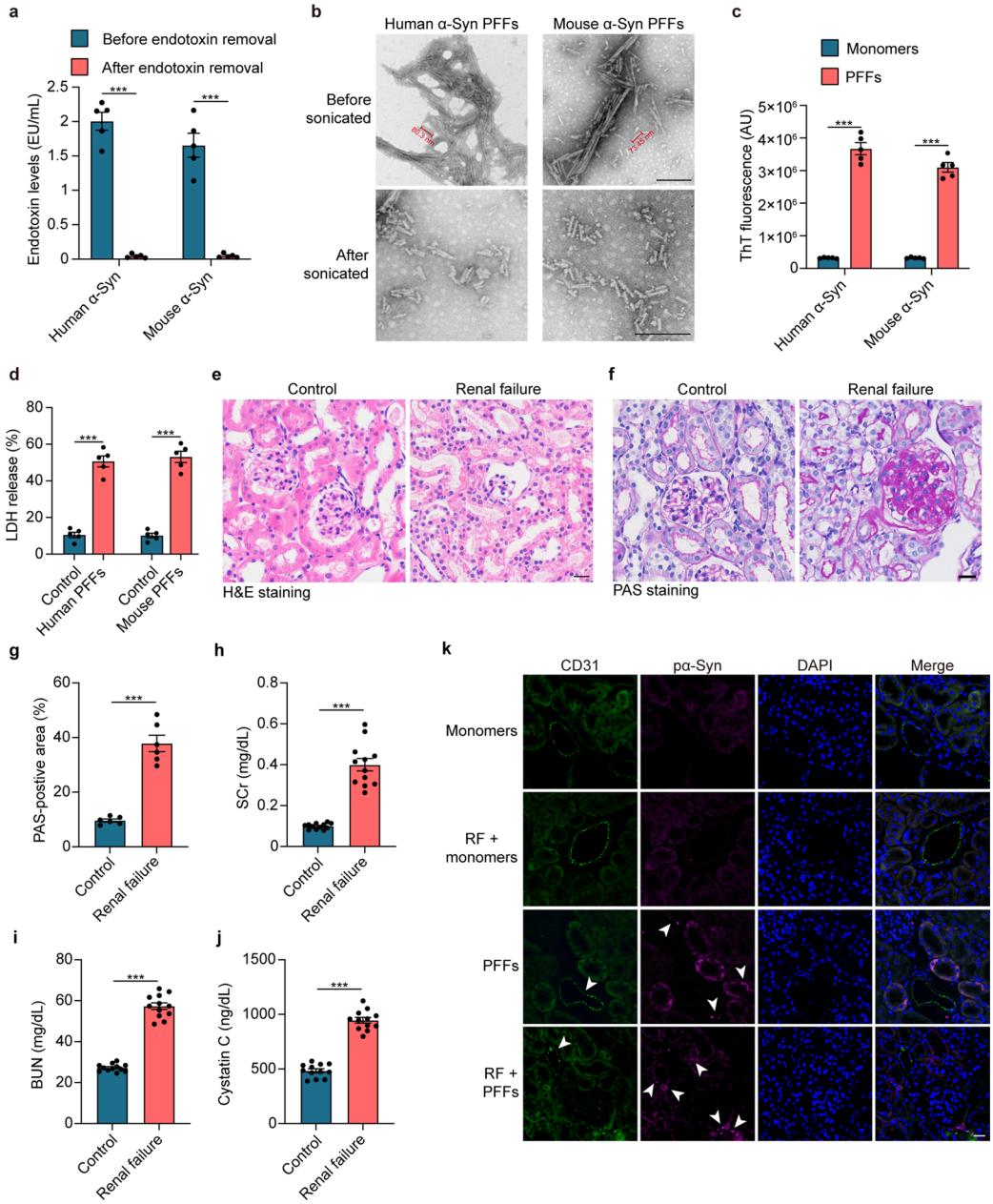

Extended Data Fig. 3 | Validation of α-Syn PFFs and evaluation of the renal function of mice with renal failure. a, Endotoxin levels of recombinant α-Syn before and after removal of endotoxin (n = 5 independent experiments; $P < 0.0001$). **b**, Transmission electron microscopy (TEM) analysis of human and mouse α-Syn preformed fibrils (PFFs) before and after sonication. **c**, ThT analysis showing the fibrillization of α-Syn PFFs used in the experiments. **d,** LDH release of the primary cortical neurons incubated with human or mouse α-Syn PFFs (n = 5 independent experiments; $P < 0.0001$). **e**, H&E staining of the kidneys. **f**,**g**, PAS staining (**f**) and quantification (**g**) of the kidneys. **h**, The serum creatinine (SCr) levels of mice with or without renal failure (n = 12 mice per group; $P < 0.0001$). **i**, The blood urea nitrogen (BUN) levels of mice with or without renal failure (n = 12 mice per group; $P < 0.0001$). **j**, The blood cystatin C levels of mice with or without renal failure (n = 12 mice per group; $P < 0.0001$). **k**, Double immunofluorescence of CD31 and pα-Syn in the kidneys of control mice or mice with renal failure that were injected with α-Syn monomers or PFFs (arrowheads: CD31-positive signals (green) and pα-Syn-positive signals (magenta)). Error bars indicate the mean ± s.e.m. ***$P < 0.001$. Unpaired two-tailed Student's t-test was used. Scale bar: 200 nm (**b**) and 20 μm (**e**,**f**,**k**).

https://doi.org/10.1038/s41593-024-01866-2

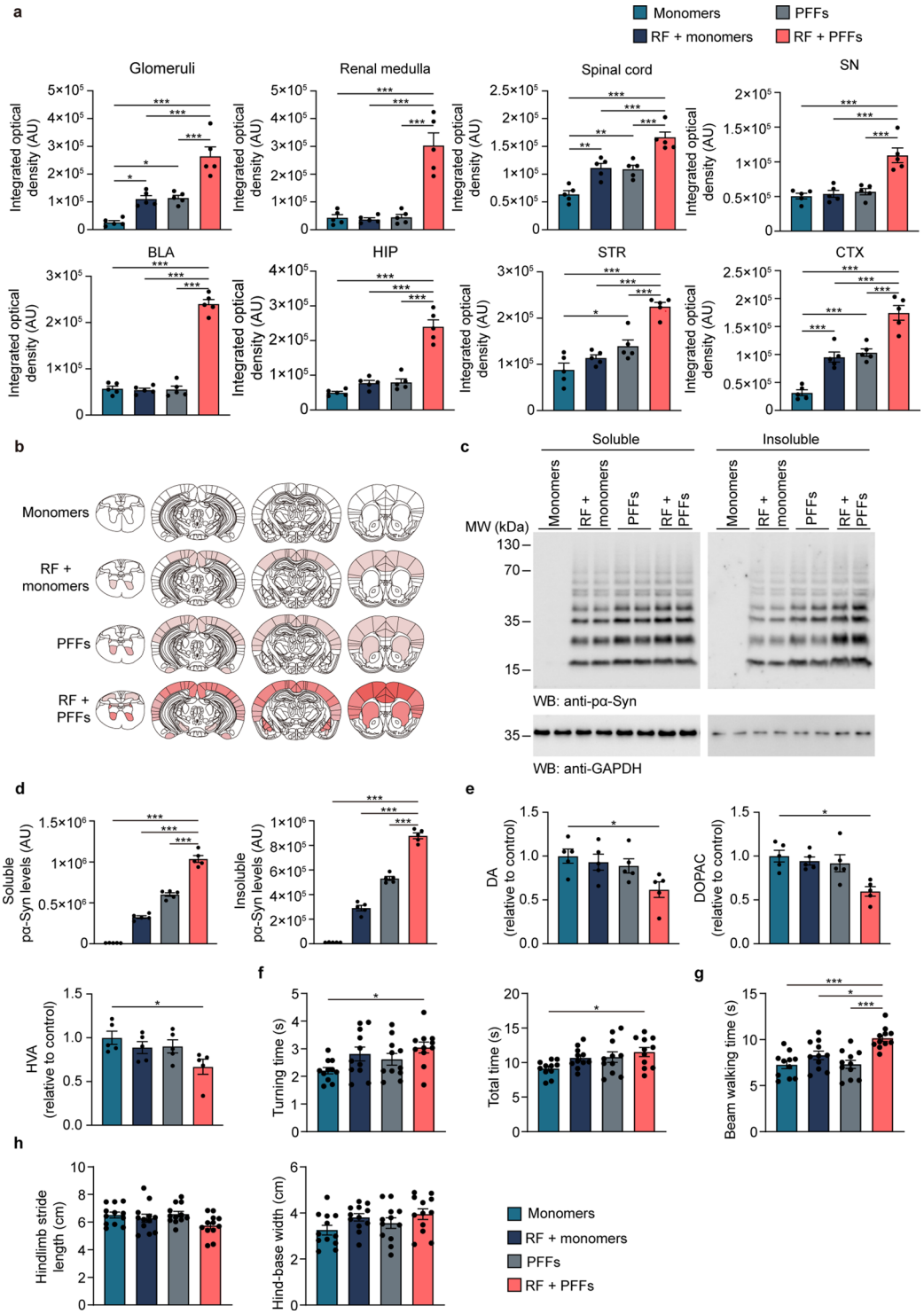

Extended Data Fig. 4 | See next page for caption.

https://doi.org/10.1038/s41593-024-01866-2

Extended Data Fig. 4 | Renal failure exacerbates α-Syn pathology induced by intravenous injection of α-Syn PFFs. a, Quantification of immunohistochemistry in Fig. 3b showing the levels of pα-Syn in the glomeruli, renal medulla, spinal cord, substantia nigra (SN), basolateral amygdala (BLA), hippocampus (HIP), striatum (STR) and cortex (CTX) of control mice or mice with renal failure that were injected with α-Syn monomers or PFFs (n = 5 mice per group; $P = 0.0255$ (glomeruli, monomers vs. RF + monomers), $P = 0.0193$ (glomeruli, monomers vs. PFFs), $P = 0.0001$ (glomeruli, RF + monomers vs. RF + PFFs), $P = 0.0002$ (glomeruli, PFFs vs. RF + PFFs), $P = 0.0028$ (spinal cord, monomers vs. RF + monomers), $P = 0.0042$ (spinal cord, monomers vs. PFFs), $P = 0.0007$ (spinal cord, RF + monomers vs. RF + PFFs), $P = 0.0005$ (spinal cord, PFFs vs. RF + PFFs), $P = 0.0001$ (SN, RF + monomers vs. RF + PFFs), $P = 0.0002$ (SN, PFFs vs. RF + PFFs), $P = 0.0267$ (STR, monomers vs. PFFs), $P = 0.0003$ (STR, PFFs vs. RF + PFFs), $P = 0.0007$ (CTX, monomers vs. RF + monomers), $P = 0.0002$ (CTX, monomers vs. PFFs), $P = 0.0002$ (CTX, PFFs vs. RF + PFFs), $P < 0.0001$ (glomeruli: monomers vs. RF + PFFs, renal medulla, spinal cord: monomers vs. RF + PFFs, SN: monomers vs. RF + PFFs, BLA, HIP, STR: monomers vs. RF + PFFs, CTX: monomers vs. RF + PFFs, RF + monomers vs. RF + PFFs)). **b**, Heatmap showing the propagation of α-Syn inclusions in the brains of control mice or mice with renal failure that were injected with α-Syn monomers or PFFs. The image represents the average pathology of 5 mice per group. **c**,**d**, Western blot analysis of the pα-Syn antibody in the ventral midbrain of control mice or mice with renal failure that were injected with α-Syn monomers or PFFs (n = 5 mice per group; $P < 0.0001$). **e**, HPLC analysis of DA, DOPAC and HVA in the striatum of control mice or mice with renal failure that were injected with α-Syn monomers or PFFs (n = 5 mice per group; $P = 0.0327$ (DA), $P = 0.0197$ (DOPAC), $P = 0.0452$ (HVA)). **f**–**h**, Behavioral test results. Pole test (**f**), beam-walking test (**g**) and footprint test (**h**) (n = 12 mice per group; $P = 0.0257$ (**f**, left), $P = 0.0263$ (**f**, right), $P = 0.0152$ (**g**, RF + monomers vs. RF + PFFs), $P < 0.0001$ (**g**, monomers vs. RF + PFFs), $P = 0.0001$ (**g**, PFFs vs. RF + PFFs), $P = 0.1122$ (**h**, left, monomers vs. RF + PFFs), $P = 0.3859$ (**h**, left, RF + monomers vs. RF + PFFs), $P = 0.0729$ (**h**, left, PFFs vs. RF + PFFs), $P = 0.1035$ (**h**, right, monomers vs. RF + PFFs), $P = 0.9640$ (**h**, right, RF + monomers vs. RF + PFFs), $P = 0.5515$ (**h**, right, PFFs vs. RF + PFFs)). Error bars indicate the mean ± s.e.m. $^{*}P < 0.05$, $^{**}P < 0.01$, $^{***}P < 0.001$. For **a**, **b**, **f**, **g** and **h**, one-way ANOVA was used. For **e**, the Kruskal–Wallis test was used. AU, arbitrary units.

https://doi.org/10.1038/s41593-024-01866-2

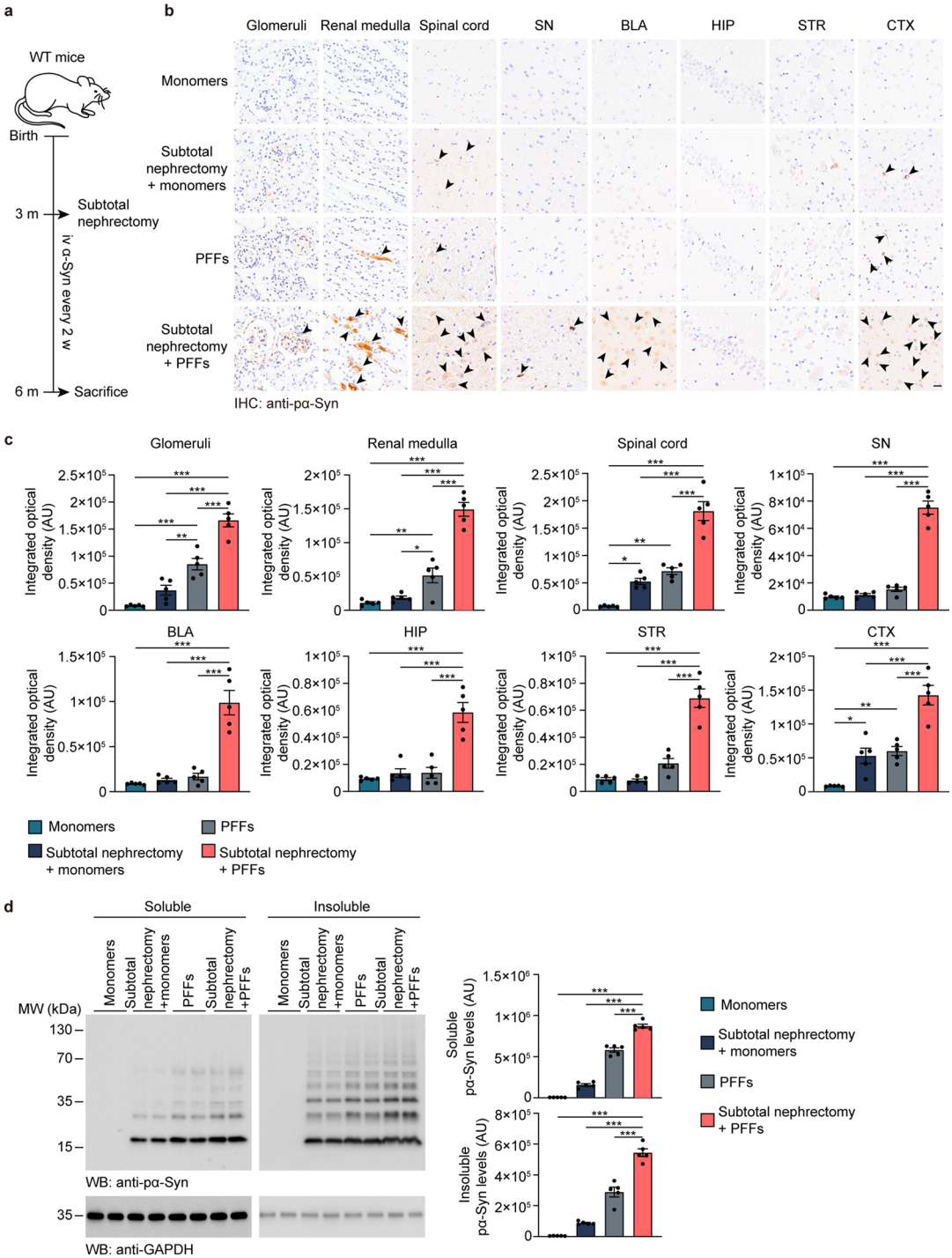

Extended Data Fig. 5 | Subtotal nephrectomy exacerbates α-Syn pathology. **a**, Timeline of the experiments. **b**,**c**, Immunohistochemistry of pα-Syn in the glomeruli, spinal cord, substantia nigra (SN), basolateral amygdala (BLA), hippocampus (HIP), striatum (STR) and cortex (CTX) of control mice or mice with subtotal nephrectomy that were injected with α-Syn monomers or PFFs ($P = 0.0001$ (glomeruli, monomers vs. PFFs), $P = 0.0096$ (glomeruli, subtotal nephrectomy + monomers vs. PFFs), $P = 0.0083$ (renal medulla, monomers vs. PFFs), $P = 0.0338$ (renal medulla, subtotal nephrectomy + monomers vs. PFFs), $P = 0.0190$ (spinal cord, monomers vs. subtotal nephrectomy + monomers), $P = 0.0011$ (spinal cord, monomers vs. PFFs), $P = 0.0237$ (CTX, monomers vs. subtotal nephrectomy + monomers), $P = 0.0084$ (CTX, monomers vs. PFFs), $P = 0.0001$ (CTX, PFFs vs. subtotal nephrectomy + PFFs), $P < 0.0001$ (glomeruli: monomers vs. subtotal nephrectomy + PFFs, subtotal nephrectomy + monomers vs. subtotal nephrectomy + PFFs, PFFs vs. subtotal nephrectomy + PFFs, renal medulla: monomers vs. subtotal nephrectomy + PFFs, subtotal nephrectomy + monomers vs. subtotal nephrectomy + PFFs, PFFs vs. subtotal nephrectomy + PFFs, spinal cord: monomers vs. subtotal nephrectomy + PFFs, subtotal nephrectomy + monomers vs. subtotal nephrectomy + PFFs, PFFs vs. subtotal nephrectomy + PFFs, SN, BLA, HIP, STR, CTX: monomers vs. subtotal nephrectomy + PFFs, subtotal nephrectomy + monomers vs. subtotal nephrectomy + PFFs)). **d**, Western blot analysis of pα-Syn in the brain cortex of control mice or mice with subtotal nephrectomy that were injected with α-Syn monomers or PFFs ($P < 0.0001$). Error bars indicate the mean ± s.e.m. $^{*}P < 0.05$, $^{**}P < 0.01$, $^{***}P < 0.001$. n = 5 mice per group, one-way ANOVA was used. Scale bars: 20 μm.

https://doi.org/10.1038/s41593-024-01866-2

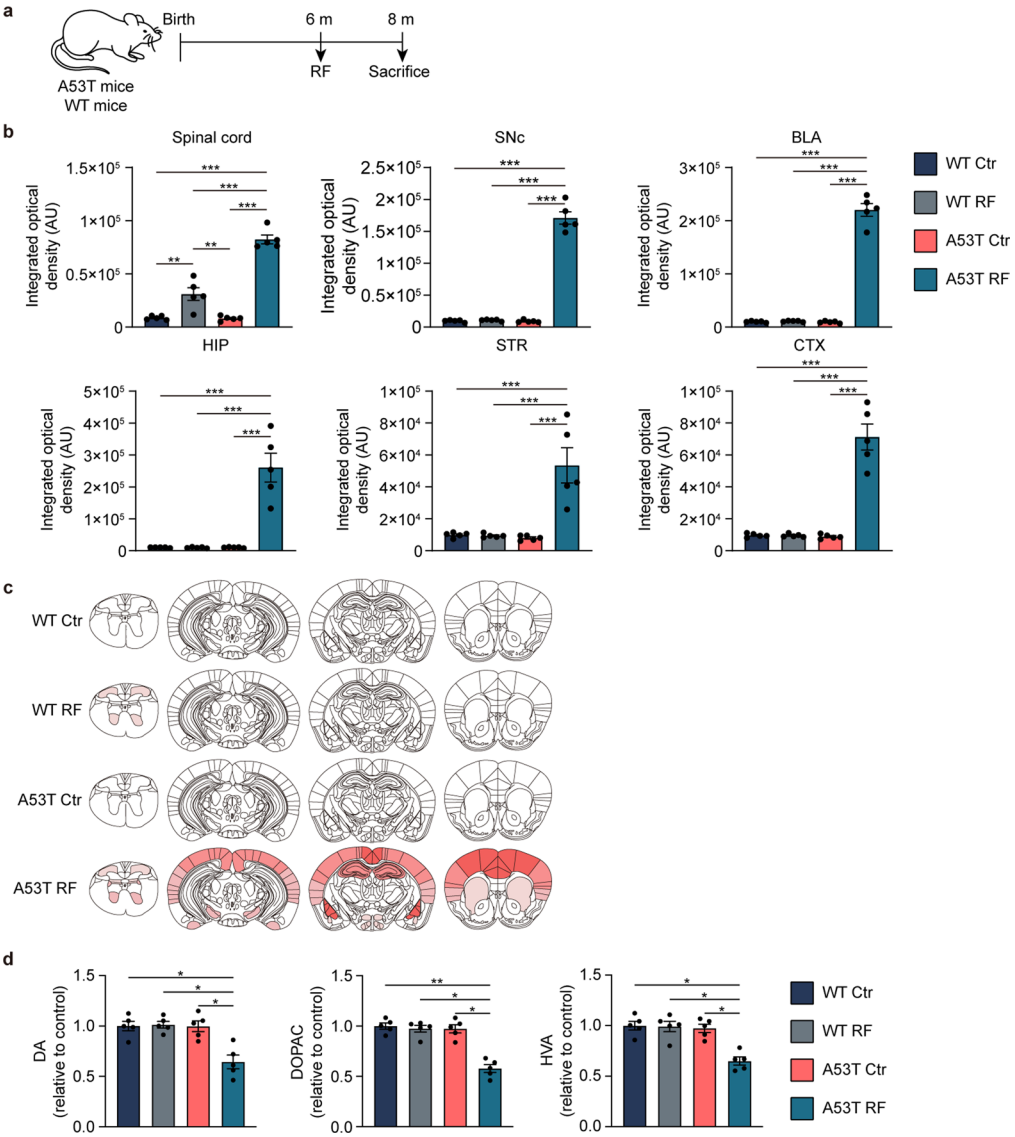

Extended Data Fig. 6 | Renal failure promotes α-Syn pathology in α-Syn A53T mice. a, Timeline of the experiments. **b**, Quantification of immunohistochemistry in Fig. 4a showing the levels of pα-Syn in the spinal cord, substantia nigra compacta (SNc), basolateral amygdala (BLA), hippocampus (HIP), striatum (STR) and cortex (CTX) of wild-type or α-Syn A53T mice with or without renal failure ($P = 0.0032$ (spinal cord, WT Ctr vs. WT RF), $P = 0.0025$ (spinal cord, WT RF vs. A53T Ctr), $P = 0.0002$ (STR, WT Ctr vs. A53T RF), $P = 0.0002$ (STR, WT RF vs. A53T RF), $P = 0.0001$ (STR, A53T Ctr vs. A53T RF), $P < 0.0001$ (spinal cord: WT Ctr vs. A53T RF, WT RF vs. A53T RF, SNc, BLA, HIP, CTX)). **c**, Heatmap showing the extent of α-Syn pathology in the brains of α-Syn A53T mice with or without renal failure. **d**, HPLC analysis of DA, DOPAC and HVA in the striatum of wild-type or α-Syn A53T mice with or without renal failure (DA: $P = 0.0485$ (WT Ctr vs. A53T RF), $P = 0.0264$ (WT RF vs. A53T RF), $P = 0.0309$ (A53T Ctr vs. A53T RF), DOPAC: $P = 0.0099$ (WT Ctr vs. A53T RF), $P = 0.0309$ (WT RF vs. A53T RF), $P = 0.0360$ (A53T Ctr vs. A53T RF), HVA: $P = 0.0176$ (WT Ctr vs. A53T RF), $P = 0.0149$ (WT RF vs. A53T RF), $P = 0.0416$ (A53T Ctr vs. A53T RF)). Error bars indicate the mean ± s.e.m. $^{*}P < 0.05$, $^{**}P < 0.01$, $^{***}P < 0.001$, n = 5 mice per group. For **b**, one-way ANOVA. For **d**, the Kruskal–Wallis test was used. AU, arbitrary units.

https://doi.org/10.1038/s41593-024-01866-2

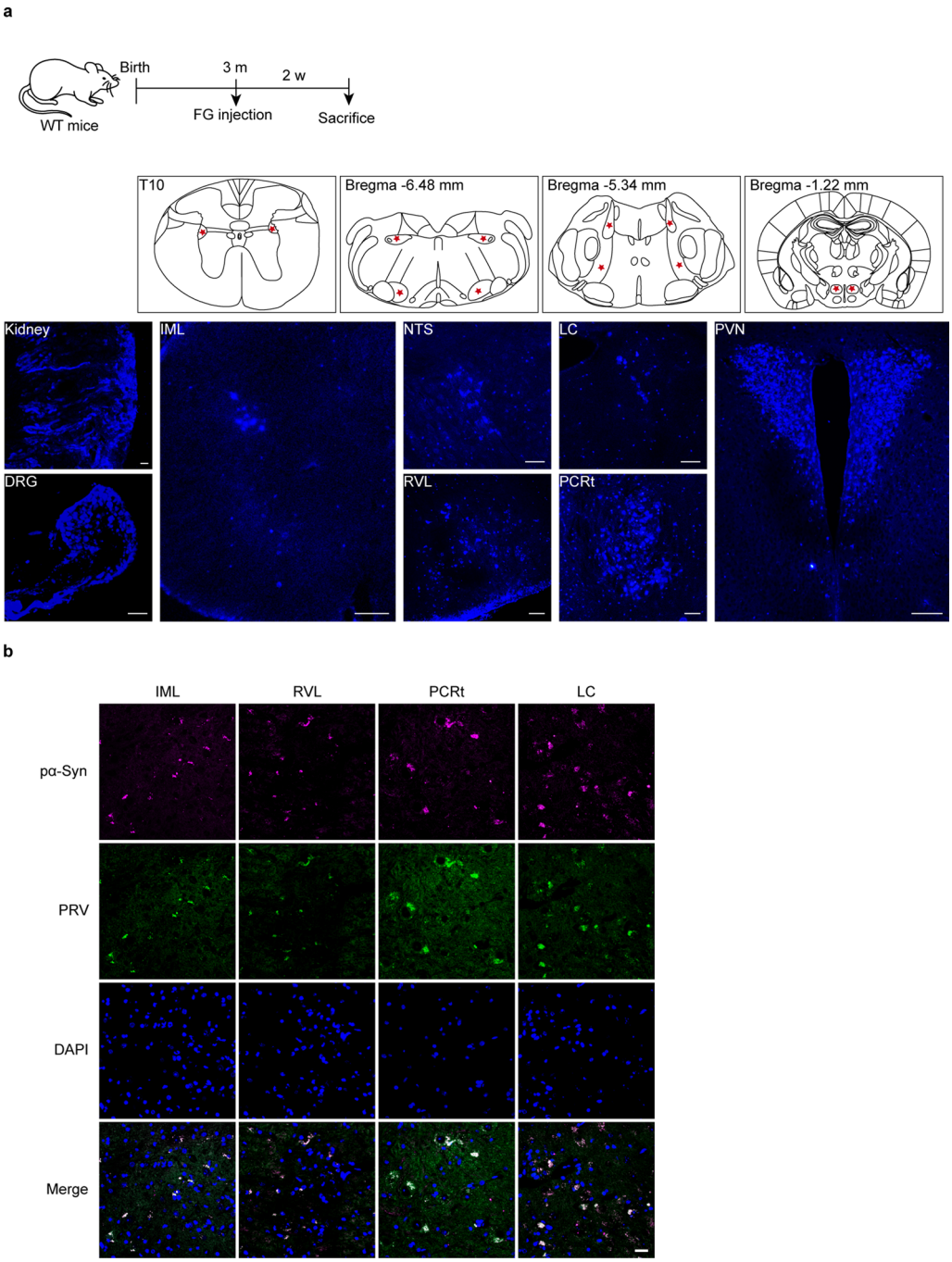

Extended Data Fig. 7 | α-Syn spreads through kidney–brain neuronal pathways. a, Representative images and schematic diagram of FG-labeled neural pathways innervating the kidney. **b**, Immunohistochemistry of pα-Syn in α-Syn A53T mice injected with α-Syn PFFs and PRV. DRG, dorsal root ganglia; IML, intermediolateral nucleus; NTS, solitary tract; RVL, rostroventrolateral reticular nucleus; LC, locus coeruleus; PCRt, parvicellular reticular nucleus; PVN, paraventricular nucleus. Scale bars: 100 μm (**a**) and 20 μm (**b**).

https://doi.org/10.1038/s41593-024-01866-2

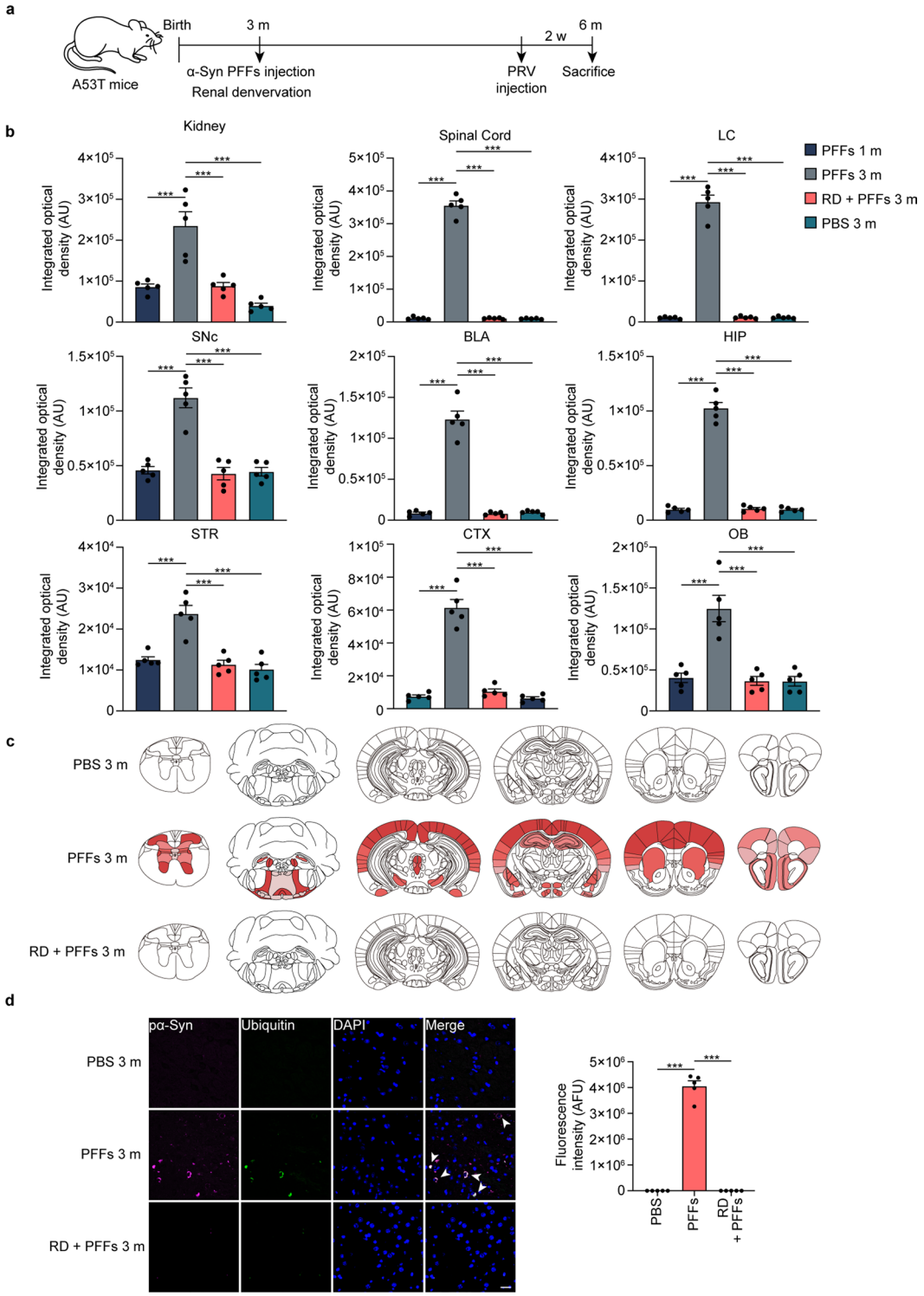

Extended Data Fig. 8 | Intrarenal injection of α-Syn PFFs promotes α-Syn pathology in α-Syn A53T mice detected by pα-Syn antibody. a, Timeline of the experiments. **b**, Quantification of immunohistochemistry in Fig. 5a showing the levels of pα-Syn in the kidney, spinal cord, locus coeruleus (LC), substantia nigra compacta (SNc), basolateral amygdala (BLA), hippocampus (HIP), striatum (STR), cortex (CTX) and olfactory bulb (OB) of α-Syn A53T mice that received intrarenal injection of PBS or α-Syn PFFs ($P < 0.0001$). RD, renal denervation; AU, arbitrary units. **c**, Heatmap showing the propagation of α-Syn inclusions in the brain of α-Syn A53T mice that received intrarenal injection of PBS or α-Syn PFFs. **d**, Double immunofluorescence of ubiquitin and pα-Syn in the striatum ($P < 0.0001$). Error bars indicate the mean ± s.e.m. ***$P < 0.001$. n = 5 mice per group, one-way ANOVA was used. AFU, arbitrary fluorescence units. Scale bars: 20 μm.

https://doi.org/10.1038/s41593-024-01866-2

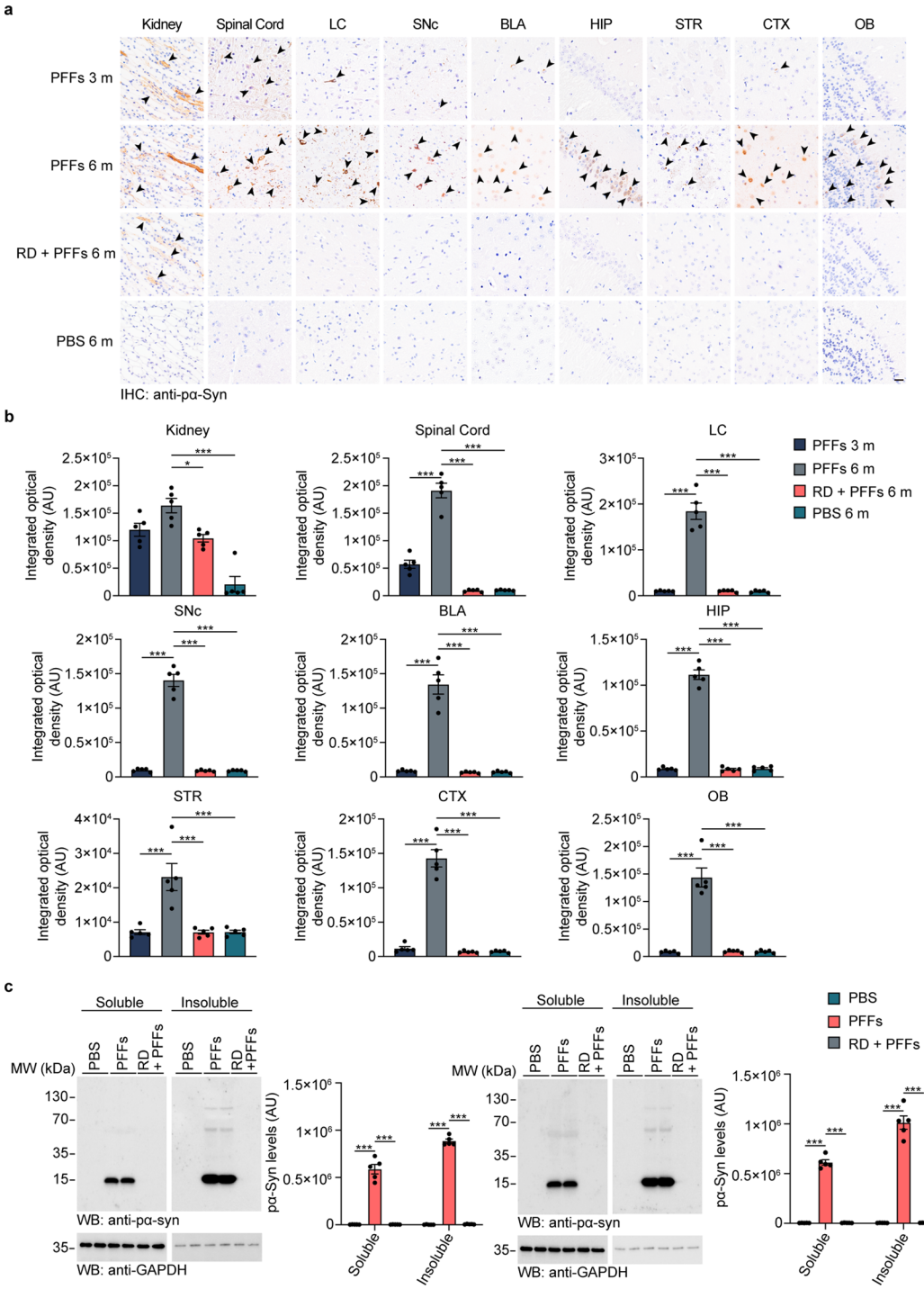

Extended Data Fig. 9 | Intrarenal injection of α-Syn PFFs promotes α-Syn pathology in wild-type mice. a,**b**, Immunohistochemistry of pα-Syn in the kidney, spinal cord, locus coeruleus (LC), substantia nigra compacta (SNc), basolateral amygdala (BLA), hippocampus (HIP), striatum (STR), cortex (CTX) and olfactory bulb (OB) of wild-type mice that received intrarenal injection of PBS or α-Syn PFFs ($P = 0.0124$ (kidney, PFFs 6m vs. RD + PFFs 6m), $P = 0.0002$ (STR), $P < 0.0001$ (kidney: PFFs 6m vs. PBS 6m, spinal cord, LC, SNc, BLA, HIP, CTX, OB)). Arrowheads: pα-Syn-positive signals. **c**, Western blot analysis of pα-Syn in the RIPA-soluble and RIPA-insoluble fractions of the spinal cord (left) and cortex (right) of wild-type mice injected with PBS or α- PFFs, respectively ($P < 0.0001$). Error bars indicate the mean ± s.e.m. $^{*}P < 0.05$, $^{***}P < 0.001$. n = 5 mice per group, one-way ANOVA was used. AU, arbitrary units; RD, renal denervation. Scale bars: 20 μm.

https://doi.org/10.1038/s41593-024-01866-2

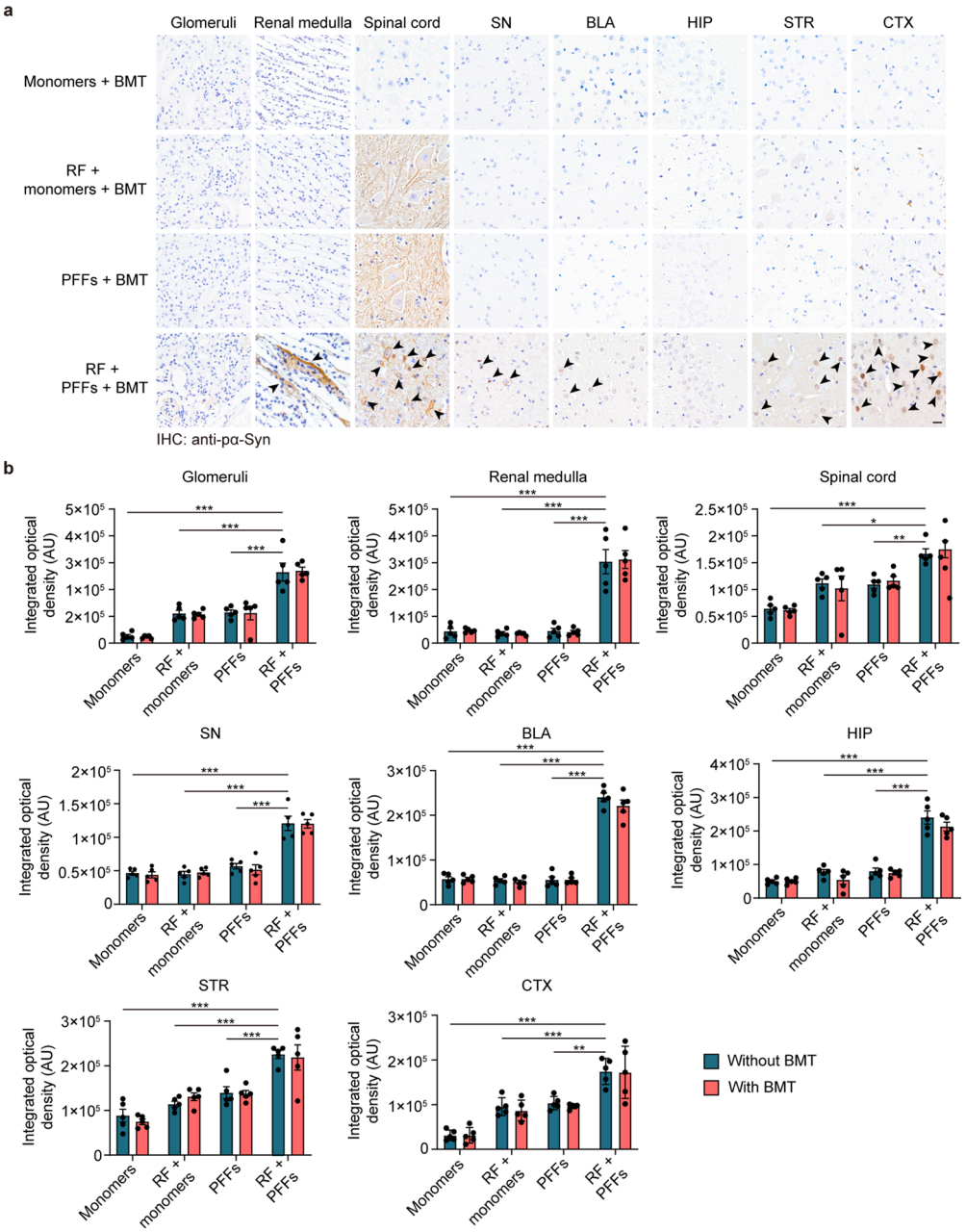

Extended Data Fig. 10 | Transplantation with Snca$^{-/-}$ bone marrow failed to reverse α-Syn pathology in mice that received intravenous injection of α-Syn PFFs. a, Immunohistochemistry of pα-Syn in the glomeruli, spinal cord, basolateral amygdala (BLA), hippocampus (HIP), striatum (STR) and cortex (CTX) of control mice or mice with renal failure that were injected with α-Syn monomers or PFFs after being transplanted with bone marrow of *Snca*$^{-/-}$ mice. Arrowheads: pα-Syn-positive signals. **b**, Quantification of pα-Syn pathology in the mouse brain. The data without BMT are the same as those in Extended Data Fig. 4a ($P = 0.0110$ (spinal cord, without BMT, RF + monomers vs. RF + PFFs), $P = 0.0078$ (spinal cord, without BMT, PFFs vs. RF + PFFs), $P < 0.0001$ (spinal cord, without BMT, monomers vs. RF + PFFs), $P = 0.0005$ (STR, without BMT, PFFs vs. RF + PFFs), $P < 0.0001$ (STR, without BMT: monomers vs. RF + PFFs, RF + monomers vs. RF + PFFs), $P = 0.0004$ (CTX, without BMT, RF + monomers vs. RF + PFFs), $P = 0.0014$ (CTX, without BMT, PFFs vs. RF + PFFs), $P < 0.0001$ (CTX, without BMT: monomers vs. RF + PFFs), $P < 0.0001$ (glomeruli, renal medulla, SN, BLA, HIP)). Error bars indicate the mean ± s.e.m. $^{*}P < 0.05$, $^{**}P < 0.01$, $^{***}P < 0.001$. n = 5 mice per group, two-way ANOVA was used. AU, arbitrary units; BMT, bone marrow transplantation. Scale bars: 20 µm.

nature portfolio

Corresponding author(s): DBRP NN-A81031C-Z

Last updated by author(s): Oct 20, 2024

Reporting Summary

Nature Portfolio wishes to improve the reproducibility of the work that we publish. This form provides structure for consistency and transparency in reporting. For further information on Nature Portfolio policies, see our Editorial Policies and the Editorial Policy Checklist.

Statistics

For all statistical analyses, confirm that the following items are present in the figure legend, table legend, main text, or Methods section.

n/a	Confirmed
☐	☒ The exact sample size (*n*) for each experimental group/condition, given as a discrete number and unit of measurement
☐	☒ A statement on whether measurements were taken from distinct samples or whether the same sample was measured repeatedly
☐	☒ The statistical test(s) used AND whether they are one- or two-sided *Only common tests should be described solely by name; describe more complex techniques in the Methods section.*
☐	☒ A description of all covariates tested
☐	☒ A description of any assumptions or corrections, such as tests of normality and adjustment for multiple comparisons
☐	☒ A full description of the statistical parameters including central tendency (e.g. means) or other basic estimates (e.g. regression coefficient) AND variation (e.g. standard deviation) or associated estimates of uncertainty (e.g. confidence intervals)
☐	☒ For null hypothesis testing, the test statistic (e.g. *F*, *t*, *r*) with confidence intervals, effect sizes, degrees of freedom and *P* value noted *Give P values as exact values whenever suitable.*
☒	☐ For Bayesian analysis, information on the choice of priors and Markov chain Monte Carlo settings
☒	☐ For hierarchical and complex designs, identification of the appropriate level for tests and full reporting of outcomes
☒	☐ Estimates of effect sizes (e.g. Cohen's *d*, Pearson's *r*), indicating how they were calculated

Our web collection on statistics for biologists contains articles on many of the points above.

Software and code

Policy information about availability of computer code

Data collection	Spectra Max plate reader (Molecular Devices, Sunnyvale, CA), Olympus DP80 microscope equipped with TH4-200 and U-HGLGPS light sources, ImageJ software (version 2.1.0/1.53c), Rotarod apparatus (MED-Associates)
Data analysis	GraphPad Prism (version 8.0), ImageJ software (version 2.1.0/1.53c)

For manuscripts utilizing custom algorithms or software that are central to the research but not yet described in published literature, software must be made available to editors and reviewers. We strongly encourage code deposition in a community repository (e.g. GitHub). See the Nature Portfolio guidelines for submitting code & software for further information.

Data

Policy information about availability of data

All manuscripts must include a data availability statement. This statement should provide the following information, where applicable:

- Accession codes, unique identifiers, or web links for publicly available datasets
- A description of any restrictions on data availability
- For clinical datasets or third party data, please ensure that the statement adheres to our policy

No datasets were generated or analysed during the current study.

Research involving human participants, their data, or biological material

Policy information about studies with human participants or human data. See also policy information about sex, gender (identity/presentation), and sexual orientation and race, ethnicity and racism.

Reporting on sex and gender	This study includes 20 males and 26 females.
Reporting on race, ethnicity, or other socially relevant groupings	This study did not involve race, ethnicity, or other socially relevant groupings.
Population characteristics	For this study, we used kidney, brain tissue, gastrointestinal tract samples, and blood samples collected from the Johns Hopkins Hospital Autopsy Service database, including 11 Lewy body disease cases (age ranged from 67 to 92 years), 37 CKD cases (age ranged from 26 to 65 years), and 30 controls (age ranged from 26 to 71 years).
Recruitment	Lewy body disease cases were selected with the following inclusion criteria: (1) subjects had been evaluated and followed by a movement disorder specialist in the Johns Hopkins Parkinson's Disease and Movement Disorder Center and had confirmed clinical diagnosis of either Parkinson's disease or Dementia with Lewy bodies; (2) confirmed neuropathological diagnosis of Lewy body disease pathology; (3) adequate paraffin embedded tissue available from brain, kidney, adrenal gland, large intestine, small intestine, stomach and esophagus. All the CKD cases fulfilled the following inclusion criteria: (1) age under 60 years old; (2) history of CKD over 3 years; (3) pathologically confirmed end stage renal disease changes; (4) no history record of neurological disorders; (5) neuropathologically unremarkable brain except having atherosclerosis and hypoxic-ischemic changes. All the control cases had no medical history of neurological disorders or renal disease and pathological examinations of both brain and kidney were unremarkable.
Ethics oversight	This study was approved by the Institutional Review Board (IRB00101384). All patients or their proxies provided written informed consent before participating in any research activity.

Note that full information on the approval of the study protocol must also be provided in the manuscript.

Field-specific reporting

Please select the one below that is the best fit for your research. If you are not sure, read the appropriate sections before making your selection.

☒ Life sciences ☐ Behavioural & social sciences ☐ Ecological, evolutionary & environmental sciences

For a reference copy of the document with all sections, see nature.com/documents/nr-reporting-summary-flat.pdf

Life sciences study design

All studies must disclose on these points even when the disclosure is negative.

Sample size	No statistical methods were used to predetermine sample sizes, but our sample sizes were similar to those generally employed in the field.
Data exclusions	No data points were excluded from statistical analysis.
Replication	We replicated the experiments three times at least, achieving similar results and standard deviations were within expected ranges.
Randomization	The mice were randomized into different groups by using a random number table.
Blinding	Investigators were blinded to the group allocation during the data collection and analyses.

Reporting for specific materials, systems and methods

We require information from authors about some types of materials, experimental systems and methods used in many studies. Here, indicate whether each material, system or method listed is relevant to your study. If you are not sure if a list item applies to your research, read the appropriate section before selecting a response.

Materials & experimental systems

n/a	Involved in the study
☐	☒ Antibodies
☒	☐ Eukaryotic cell lines
☒	☐ Palaeontology and archaeology
☐	☒ Animals and other organisms
☐	☒ Clinical data
☒	☐ Dual use research of concern
☒	☐ Plants

Methods

n/a	Involved in the study
☒	☐ ChIP-seq
☒	☐ Flow cytometry
☒	☐ MRI-based neuroimaging

Antibodies

Antibodies used: α-Syn (1:1,000, ThermoFisher, MA5-12272), α-Syn (1: 1000, BD Biosciences, 610786), pα-Syn (1:1,000, Ser129, Biolegend, 825701), pα-Syn (1:1,000, Ser129, Cell Signaling Technology, 23706s), Syn303 (1: 1,000, Biolegend, MMS-5091), 5G4 (1: 1,000, Sigma, MABN389), TH (1:1,000, Sigma-Aldrich, AB152), DAT (1:500, Proteintech, 22524-1-AP), ubiquitin (1:1,000, Santa Cruz Biotechnology, Sc-8017), CK2α (1: 1000, Proteintech, 2656), GAPDH (1:5,000, Proteintech, 60004-1-Ig), HRP-conjugated anti-mouse IgG (1:8,000, Bio-Rad, 170-6516), HRP-conjugated anti-rabbit IgG (1:8,000, Bio-Rad, 170-6515), Alexa Fluor 594-conjugated goat anti-mouse IgG (1:500, Invitrogen, A-11005), Alexa Fluor 488-conjugated goat anti-rabbit IgG (1:500, Invitrogen, A-11012).

Validation: All antibodies were verified in mice tissue, human cell line, or primary culture cell by western blotting to ensure that the antibody binds to the antigen stated.

Animals and other research organisms

Policy information about studies involving animals; ARRIVE guidelines recommended for reporting animal research, and Sex and Gender in Research

Laboratory animals: Adult C57BL/6J mice, Snca-knockout mice, and human A53T variant α-syn transgenic line M83 were from the Jackson Laboratory (stock number: 000664, 003692 and 004479, respectively). Rabbits were purchased from Hubei Provincial Center for Disease Control and Prevention (Wuhan, China).

Wild animals: The study did not involve wild animals.

Reporting on sex: Only male animals were used in the experiments.

Field-collected samples: The study did not involve samples collected from the field.

Ethics oversight: The protocol was reviewed and approved by the Institutional Animal Care and Use Committee.

Note that full information on the approval of the study protocol must also be provided in the manuscript.

Clinical data

Policy information about clinical studies

All manuscripts should comply with the ICMJE guidelines for publication of clinical research and a completed CONSORT checklist must be included with all submissions.

Clinical trial registration: *Provide the trial registration number from ClinicalTrials.gov or an equivalent agency.*

Study protocol: *Note where the full trial protocol can be accessed OR if not available, explain why.*

Data collection: *Describe the settings and locales of data collection, noting the time periods of recruitment and data collection.*

Outcomes: *Describe how you pre-defined primary and secondary outcome measures and how you assessed these measures.*